International Journal of Earth Sciences Knowledge and Applications
journal homepage: http://www.ijeska.com/index.php/ijeska

Research Article

e-ISSN: 2687-5993

Baseline Geo-Engineering Dataset and Parameters' Empirical Modeling for Civil Engineering Construction in Okeigbo, Southwestern Nigeria

Falowo Olumuyiwa Olusola[1,2]*, Olorunda Oluwafemi[2], Ologan Tunde[2], Ayetoro Ayodeji[2]

[1]*Department of Applied Geology, Federal University of Technology Akure, Ondo State, Nigeria*
[2]*Department of Civil Engineering Technology, Faculty of Engineering Technology, Rufus Giwa Polytechnic, Owo, Ondo State, Nigeria*

INFORMATION

Article history
Received 01 July 2023
Revised 18 August 2023
Accepted 19 August 2023

Keywords
Settlement
Flexible pavement
Geotechnics
Geoinformatics
Bearing pressure

Contact
*Falowo Olumuyiwa Olusola
oluwanifemi.adeboye@yahoo.com

ABSTRACT

This study deals with development subsoil geoengineering dataset and modeling of parameters in Okeigbo area of Ondo State, Southwestern Nigeria. The study employed geophysical methods, geotechnical survey, hydrogeological, and laboratory analysis. Findings revealed the subsoil to be clayey with low compressibility and plasticity. The clay mineral group is dominantly illite-montmorrilonite, of low activity (0.36), and hydraulic conductivity of 3.67E-08 cm/s, while the plasticity index is 23.4 %. The depth to groundwater ranged from 2.2 m (in well) – 18 m (in borehole). The depth to basement rock is between 8.2 – 31.5 m (avg. 20.9 m), indicating a moderate to deep weathering profile, able to support burial of engineering utilities such as mast, transformer, gadgets. In regard to pavement construction, the soils are unsuitable for subgrade, base and sub-base courses with CBR less than 7% and GI of 14 (avg.). However, a recommended minimum thickness of 79 – 140 mm was obtained from design curves for flexible pavement. The average allowable bearing capacity of the soil for square and round foundations is 320 KN/m^2. The total settlement obtained varies between 23.92 – 29.77 mm for structural pressure of 100 KN/m^2. The embankment suitability index of the soil suggests an expanding, but not collapsible construction material. Summarily, the subsoils have very low suitability/workability index, hence poor/fair performance for roadway, foundation, canal sections, and earth fill dams. The empirical models gave correlation coefficient of: MDD/PI vs. CBR (0.0046), LL vs. coefficient of consolidation (0.0127), PI vs. undrained shear strength/effective overburden (0.0074), PI vs. angle of shearing (0.0420), dry density vs. angle of shearing (0.4022), suitability index vs. CBRs (0.0968), clay contents vs. PI (0.0777). Schist and quartzite dominated the area, having high value as foundation constructions, aggregate in pavement, and building stone, hence can be trusted in most engineering construction works.

1. Introduction

Geotechnical Investigation is very important before any structure is built (Coker, 2015; Das, 2015; Ezenwaka et al., 2014). A detailed investigation will often lead to lower risk and/or lower project overruns. No matter what structure is built it will require a geotechnical investigation to determine the soil / rock properties such as expansive nature of soil, moisture content, compressibility of soil, bearing capacity and settlement, that the structure will be founded upon (Olayanju et al., 2014; Griffiths, 2002; Hawkins, 1986). All structures are founded either on or in soil or rock and design of all engineering structures are based on material properties. Poor investigation can lead to unforeseen issues whereas a thorough investigation can minimize risks when more is known (Carter and Symons, 1989; Clayton et al., 1996). Consequently, the information provided within a soil report should assist structural engineers in designing appropriate slabs, footings, or deep foundations (if required) to ensure the structure is safe and appropriately designed i.e., less prone to cosmetic defects such as cracking (Craig, 1996). All structures are founded either on or in soil or rock and the design of all engineering structures are based on material properties.

The alarming increase in the incidences of structural collapse in Nigeria can be linked to the failure of foundation soils, apart from poor quality of construction materials in some cases (Fajana et al., 2016; Adeoti et al., 2016; Matawal, 2012). In addition, geological and groundwater conditions, and more particularly the various types of ground movement that can occur are fundamental for the sustainability of any infrastructure (Bell, 2007). Hence, these information must be incorporated into the engineering design and also inform the choice of foundation types and construction methods. Thus, failure to adequately investigate, characterize, predict and incorporate the soil profile under the entire structure, the material properties of the varying soil layers and their time dependent response to imposed structural loads into a design is automatically planning for the structure to fail (Brink et al., 1992; Adewuyi and Philips, 2018; Adejumo et al., 2015; Roy and Bhalla, 2017).

In addition, according to the sustainable development goals (SDG), the development of infrastructures (SDG 9) and cities/communities (SDG 11) has to be both resilient and sustainable (Utgard et al., 1978; Culshaw et al., 1987; Legget, 1973). Therefore, to achieve these goals, it requires predesign geotechnical studies to properly and adequately characterize: the soil material at the foundation, assess the thickness, depth of occurrence and types of foundation material; and predict structural settlement which could be differential and can cause redistribution of the load transfer mechanisms to the members founded on the weak substratum and resulting in failure.

A geotechnical investigation will often include surface exploration including a walkover survey to observe existing conditions and performance of existing structures and subsurface exploration of a site using drilling or other excavation methods (Bell, 1998; Prentice, 1990; McNally, 1998). Subsurface exploration usually involves soil sampling, in situ test and laboratory tests of the soil samples retrieved. Part of the investigation may include, In-situ probing to enable the assessment of engineering parameters of the ground: Plate bearing test, California bearing ratio., Light/Heavy weight deflectometer or Falling Weight Deflectometer (FWD), Density measurement., Standard penetration test (SPT), Dynamic penetration tests, such as the dynamic cone penetrometer – DCP, Specialized cone penetration tests, such as the static cone, piezo-cone, electrical conductivity cone, and seismic cone are also used (Douglas and Olsen, 1981; Cetin and Ozan, 2009; Moss et al., 2006; Mayne, 2007).

In addition to geotechnical investigation, geophysical surveys are also being used. The argument for this method as preliminary or supplement to site investigation are sound, thus they have in fact been used extensively, especially seismic refraction, and electrical resistivity (Rungroj and Mark, 2015; Osinowo and Falufosi, 2018; Idornigie et al., 2006). Others include self-potential, electromagnetic profiling, ground penetrating radar, and borehole logging.

The seismic refraction method is based on the fact that seismic waves travel at different velocities in different geological formations (McDowell et al., 2002; Simons et al., 2001). The electrical method makes use of three basic properties of rock: resistivity which is reciprocal of conductivity, electrochemical activity (self-potential method), and electrical storage capacity (inductive prospecting methods). The electrical resistivity (ER) logging is based on the principle that any change in the specific resistance of a rock or soil will change the flow of current through the material and thereby increase or decrease the electrical potential between two mutually displaced measuring electrodes (Sharma, 1997; Reynolds, 2004).

Resistivity is a function of the electrolyte contained in the pore spaces of the material and is inversely proportional to the porosity. In massive but fractured rocks, therefore, the spatial distribution density of the fissures directly controls the resistivity (Milson, 2002). In water – dominance feature the presence of phreatic surface can completely obliterate information concerning vertical changes in rock type. There are two most popular arrays used in electrical resistivity: Wenner and Schlumberger configurations (Fig. 1).

The Wenner array is the one most commonly used, wherein current is passed into the ground through electrodes inserted at A and B, and the associated potential gradient is measured by two secondary electrodes at M and N. The electrode spacing in this configuration is such that AM = MN = NB = one third of AB. When the electrode separation is small, very little of the induced current is able to penetrate second layer and the apparent resistivity tends to ρ_1 . The apparent resistivity can be expressed as (*Equation 1*):

$$\rho = 2\pi a \frac{V}{I} \quad (1)$$

Where a is the inter-electrode spacing, V is the measured voltage, I is the induced current. When the spacing are large compared with Z_1 the apparent resistivity tends to ρ_2 because most of the induced current penetrates to the lower layer.

The expanding electrode technique called Schlumberger was adopted for this study. In Schlumberger configuration, the spacing between the potential electrodes must not exceed 40% of the half the distance of the spacing (AB) of the current electrodes. For the Schlumberger VES array, the apparent resistivity is obtained from the *Equation 2*:

$$\rho_s = {}^{\pi RL^2}/_{2L} \quad (2)$$

In-situ geotechnics has proved very effective especially where a realistic assessment is required for structure (Bell, 2004). The most widely used penetration test is the standard penetration test in which a standard (50 mm) split-spoon sampler is driven into the ground by a series of blows from a 628 N weight falling through a height of 0.76 m. During the test, the sampler is driven to its full length of 0.46 m and the number of blows required to penetrate the final 0.30m are recorded (Rogers, 2006).

Another penetration test which is widely used in practice is the static sounding method, typified as Dutch Cone test. The

equipment for which comprises a solid cone with a 30° half angle and 0.01 m^2 cross sectional area. This is thrust into the ground by hydraulic pressure through a cylindrical casing for distance of 100 mm at a rate of 1 mm/min, and the resistance is recorded. The cone resistance measurement is normally obtained at 200 mm intervals and plotted as a depth/resistance log. There is little relationship between this log and SPT log. Thus, it is sometimes assumed that N is equal to 0.25 percent of the static cone resistance expressed in kN/m^2 (Sanglerat, 1972).

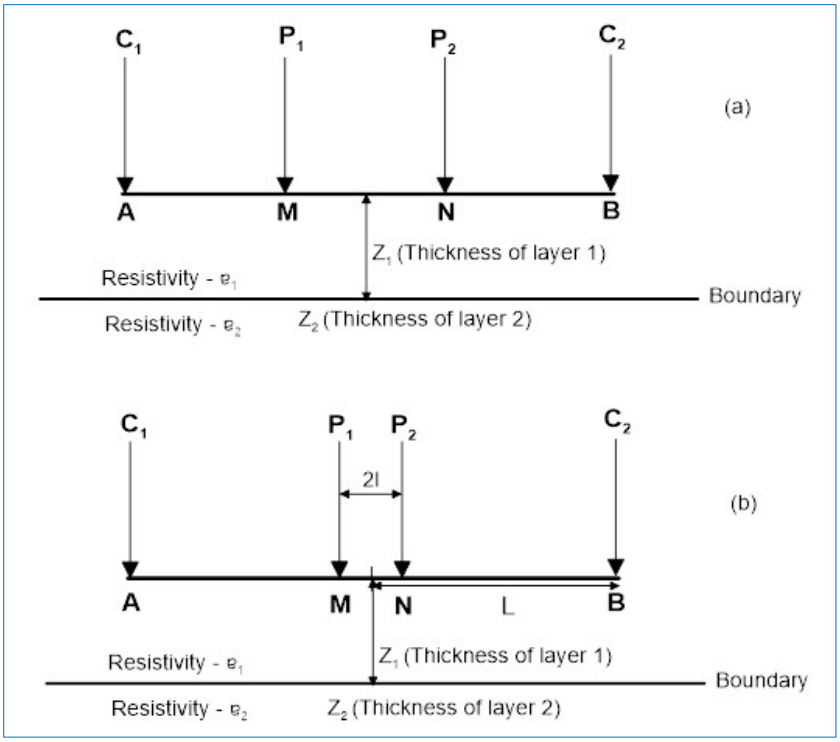

Fig. 1. Electrical resistivity Electrodes configurations (a) Wenner (b) Schlumberger

According to the ultimate aim of engineering geology is to provide information on the mechanical properties of a zone of rock or soil in order to enable an adequate and economic design to be prepared (Attewell and Farmer, 1988; Bell, 2007). According to Code of Practice for site investigation, the objectives of site investigation are to assess the general suitability of a site for proposed engineering works; to enable preparation of an adequate and economic design; to foresee and provide against geotechnical problems during and after construction; and to investigate any subsequent changes in conditions, or any failure during construction (McCann et al., 1997; Simons et al., 2001).

Consequently, the principal aim of this study is to evaluate the soil and rock conditions in Okeigbo area of Ondo State; and develop geo-engineering recommendations for design and construction for diverse civil engineering construction works such as buildings (bearing capacity and expected foundation settlement), pavement and airfields, soil excavation and workability potential, and embankments (Ojo et al., 2015; Coker, 2015; Oyedele and Olorode, 2010; Soupios et al., 2007; Lunar and Jadi, 2000; Coker et al., 2013).

The objectives include delineation of the subsurface geological sequence; determination of its geoengineering parameter (acquisition of geoelectrical, geotechnical, geochemical properties of soils for adequate and economic design of structures) and modelling; identification of geological features that could pose a threat to stability of structures; evaluation of the suitability of the subsoil and rocks within the study area for different civil engineering structures; and determination of groundwater conditions.

The information gained from this study is exceptionally vital in decision making process for choosing the appropriate design and footing of structure based on the subsurface inhomogeneity common in the basement complex of southwestern Nigeria. This study is therefore pertinent in safeguarding correctness of construction and the subsequent stability and success of structures (such as roads and airfields, embankment, and buildings) while guaranteeing protection of life and property on extended period of time.

2. Materials and Methods

2.1. Site Description

Okeigbo, which is the investigated area, is located between 689000 m and 694000 m East and 790000 m and 794500 m North of southwestern Nigeria (Fig. 2) in Ile-Oluji Local Government Area of Ondo State, Nigeria. It shares boundaries in the East with Ondo town and Ifedore Local Government Areas of Ondo State and in the west by Osun State. The town is surrounded by rocks from which it derived its name from, Oke (hills) and Igbo (forest). The climate is of

tropical rain forest characterized by wet (April to September) and dry season (October to March). The mean annual rainfall is 1500 mm, the average temperature (at peak) is 32 °C especially in February and 25 °C in August (Iloeje, 1981). The relative humility is 70% in January to 90% in July (Federal Meteorological Survey, 1982). The elevation varies between 190–270 m. The drainage pattern in the area is dendritic while groundwater is primarily recharged by precipitation and secondarily by lateral flow from rivers and their tributaries.

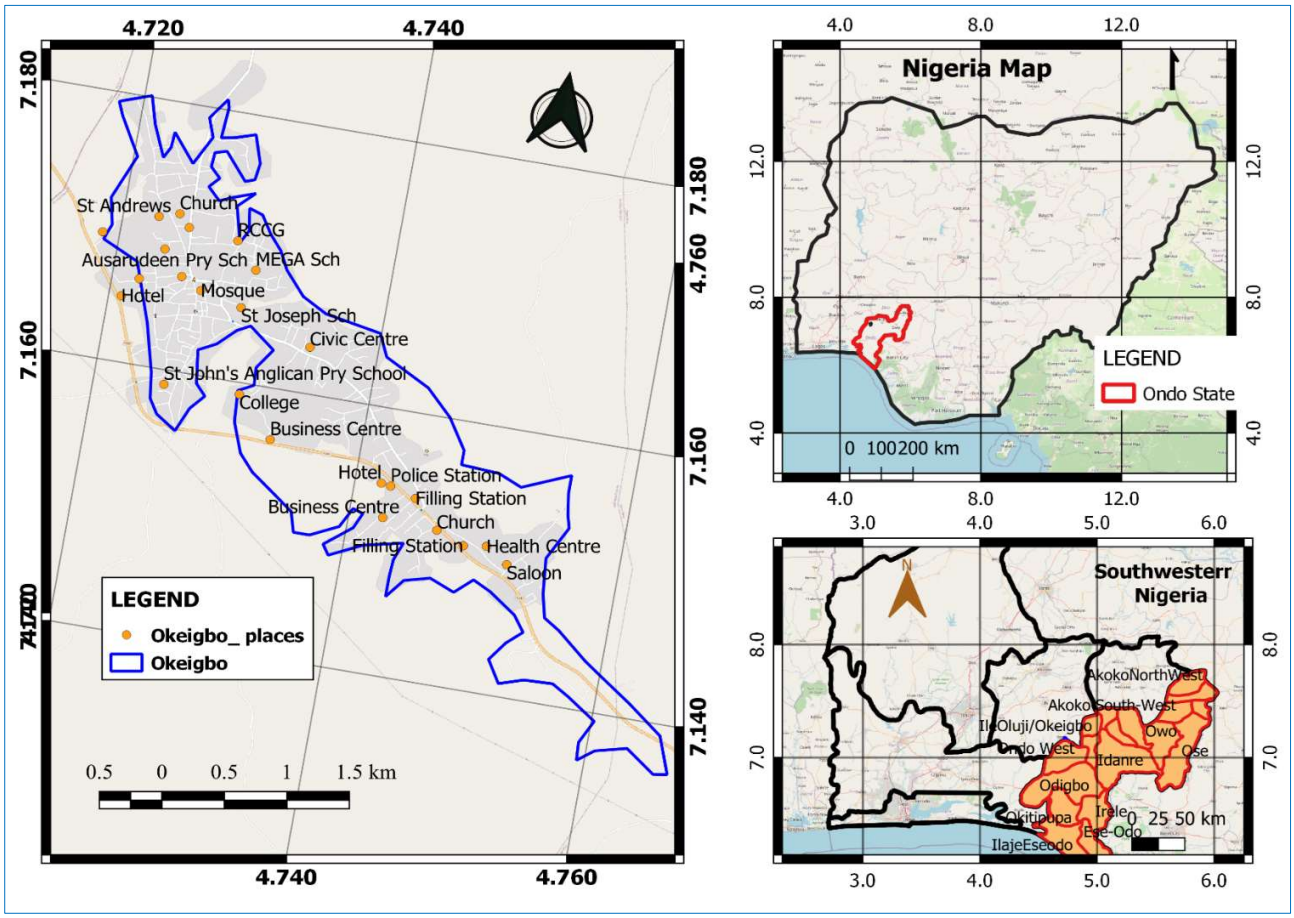

Fig. 2. Location map of Okeigbo on the maps of Ondo State and Nigeria

2.2. Geology

The geology of the area is that of the basement complex of southwestern Nigeria, with four main lithological groups, migmatite-gneiss-quartzite complex, schist belts, older granites, and minor intrusives (Figs. 3 and 4). However lithologic units observed in the area are quartzite which is flaggy, quartz metadiorite, and quartz schist. Many of the places underlying by schist and quartzite is generally concealed by a variable thick overburden which in many places are clay or laterite. Several structural features occurring on the lithologic units including joints, faults, folds, foliations, intrusions, and rock-to-rock contacts. The structural features trend in NNW-SSE and NNE-SSW. Noticeable springs (about seven) from the hills, rivers, streams, were observed in the area as one of the sources of water for the community. The major occupations of the people are agricultural and mining of sand and gravel. The local rainfall is the major recharge for the aquifer system in the area. The hydrogeologic units in the area weathered material (formed by weathering activities) and fractured basement aquifers (formed through tectonic/orogenic activities). The best groundwater potential zones are where the fractured basement underlies the weathered zone. In most basement terrain, the overburden is usually thin, and hereby makes it vulnerable to vertical source movement contamination through infiltration, leaching, and flooding.

2.3. Materials, Data Acquisition procedures and Analysis

According to the ultimate aim of engineering geology is to provide information on the mechanical properties of a zone of rock or soil in order to enable an adequate and economic design to be prepared (Attewell and Farmer, 1988; Bell, 2007). According to Code of Practice for site investigation, the objectives of site investigation are to assess the general suitability of a site for proposed engineering works; to enable preparation of an adequate and economic design; to foresee and provide against geotechnical problems during and after construction; and to investigate any subsequent changes in conditions, or any failure during construction (McCann et al., 1997; Simons et al., 2001).

Consequently, in achieving the following objectives, the

methodology adopted for this study includes preliminary investigation, field survey/measurement, and laboratory testing.

The preliminary investigation entailed study of the geology (rock units/soil), landforms, history, and relevant case histories aimed at isolating likely problems and enabling accurate planning and estimating of fieldwork. This information is usually obtained from published and private sources or records/maps, from which overall geological structure, slope angles, groundwater level and type of rock unit underlying the site can be obtained. Also, structural behavior of critical infrastructural were studied and ground condition (in terms of settlement/consolidation) in order to estimate the correctness of design. The data acquisition map for this study is presented in Fig. 5.

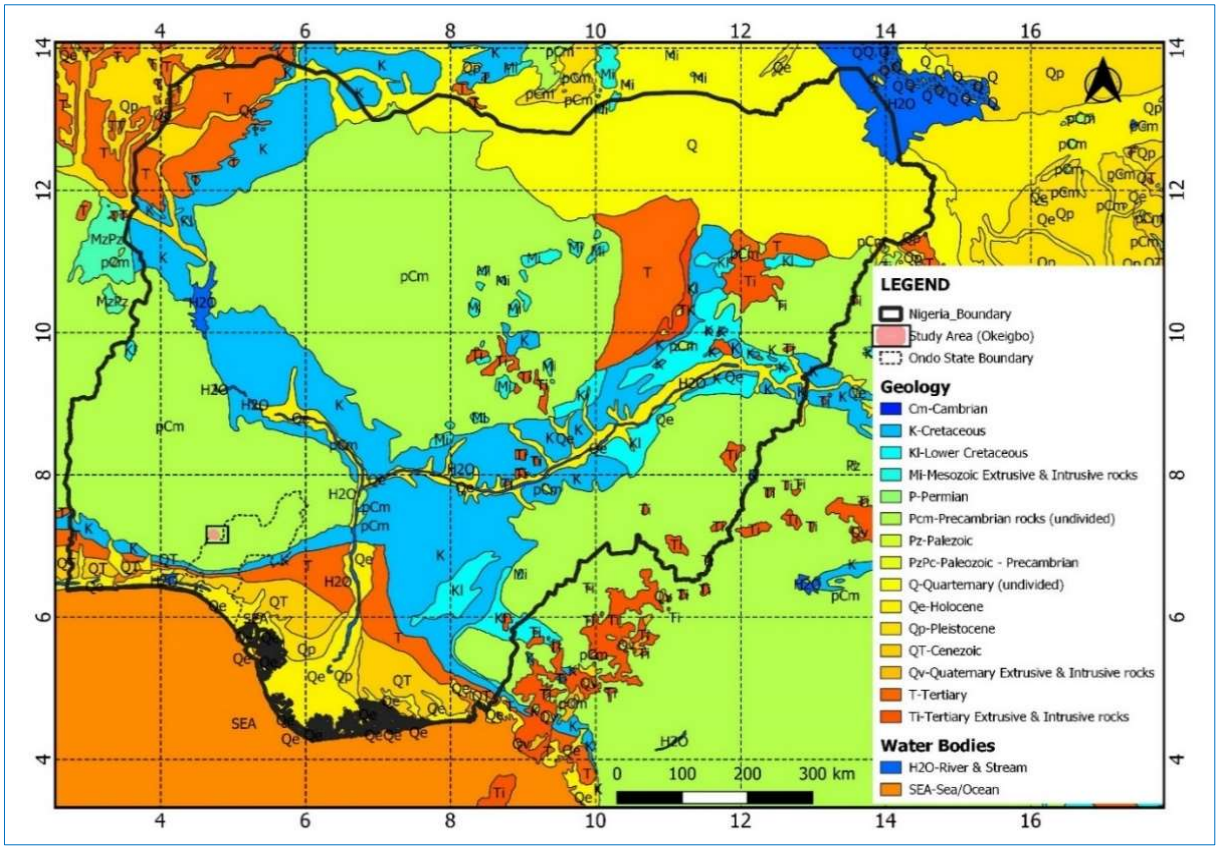

Fig. 3. Geological map of Nigeria showing the study area within the Southwestern Basement Complex (modified after NGSA, 1984)

The trial pit tends to be used for ground investigation at shallow depths in soils where they can give an accurate impression of the strata lithology, while boring is invariably used for a deeper and more extensive exploration in soils and for any subsurface exploration in rocks (Bell, 2007). For this study, 12 trial pits were dug by means of a hand–digger to a depth between 1–3 m. The excavated soil was placed about 1.0 m away from the edge of the pits. No groundwater table was observed during the exercise. The samples were collected from the pits from its sides/bottom (for disturbed sample), while tube samples were collected below the bottom of the pit (for undisturbed). The disturbed samples were collected for shear strength parameters determination and consolidation test. Immediately, the pits were examined, and samples collected, they were sand filled after use. The use of trial pits enables the in-situ soil to be examined visually, and thus the boundaries between strata and the nature of any macro-fabric can be accurately determined.

The GPS was used to take the coordinates of all sampling locations for all field surveys. The GPS is cost effective and time saving to traditional use of theodolites and levels. The geotechnical parameters were analyzed using America Standard for Testing and Material (ASTM, 2006) and British Standard (BS 1377, 1990) procedures, with the following tests: natural moisture content (D2216), grain size distribution (D422; D1140), specific gravity (D854; D5550), consistency limit and linear shrinkage (D4318),, density (BS 1377, 1990), triaxial (D4767; D2850), unconfined compressive strength (D2166), permeability (D2434), compaction (D1557; D698), California Bearing Ratio, one dimensional consolidation (D4186; D4546). The in-situ CPT test was done following ASTM-D3441-94 procedures.

The CPT equipment utilized the Dutch cone penetrometer with an anvil, driving rod, and other accessories. The machine nominal capacity was 10-tonnes and was operated by using hydraulically operated driving mechanism. The cone tip angle of the penetrometer used was 60° and rods of 100 cm long. In order to obtain the cone resistance value, the

cone was pushed vertically at a rate of 2 cm/s a depth of 0.25 m each time. Penetration resistance (q_c), sleeve friction (f_s) and the depth of penetration were recorded at each station and processed into plots.

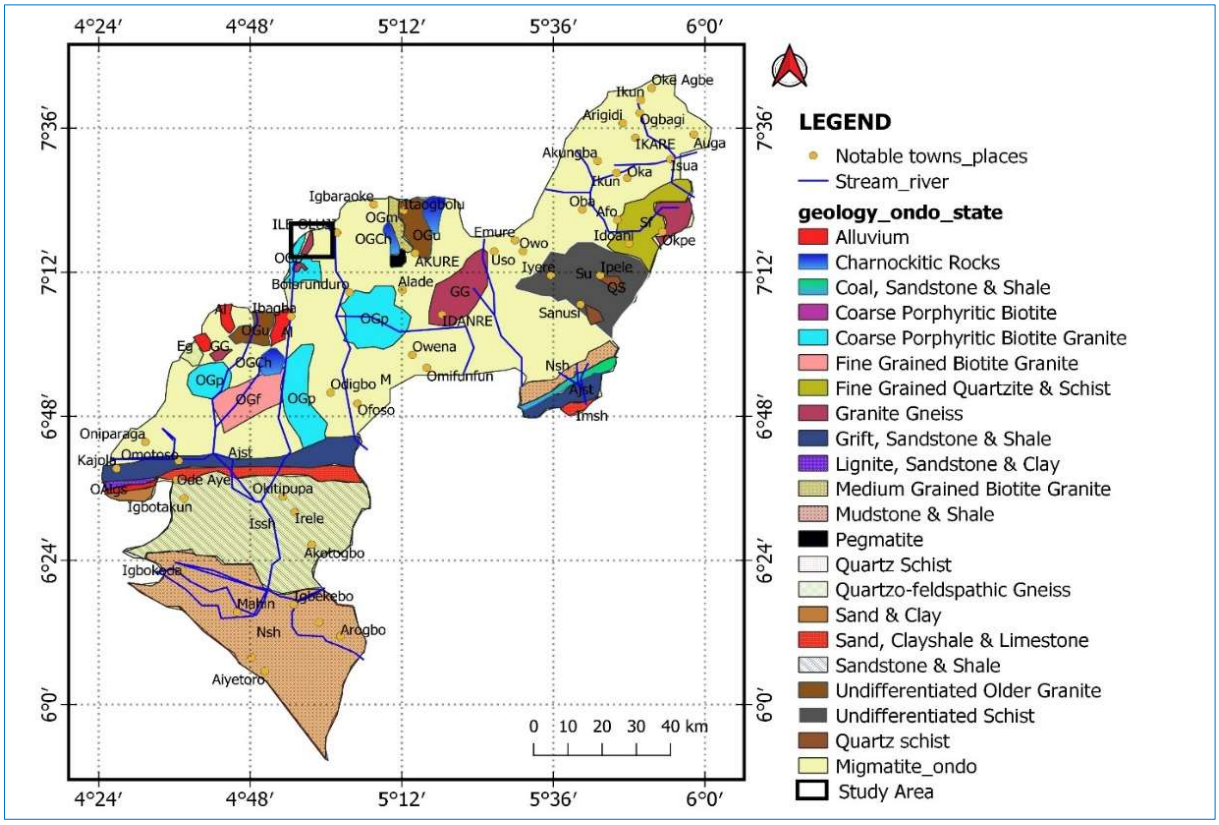

Fig. 4. Geological map of Ondo State, showing the local rock units which included Migmatite and Coarse – Porphyritic Biotite Granite (modified after NGSA, 2006)

All the test reached refusal before the anchors pulled out of the subsurface. The layer sequences were interpreted using the friction ratio (Fig. 6), while cone resistance contrast between the various layers, inflection points of the penetrometer curves were interpreted as the interface between the different lithologies (Mayne, 2007; Robertson, 1990).

Both qualitative and quantitative interpretation of the CPT readings in this study followed the guidelines of ASTM D 5778. The CPT data was normalized to standard overburden pressure (q_{cn}) of 100 KN/m^2 (Moss et al., 2006).

Hence from the result of the CPT, unconfined compressive strength (*Equation 3*), ultimate bearing capacity was derived (*Equations 4 and 5*), ultimate capacity (Q_{ult}) and elastic modulus for strip and square using *Equations 7–8*, respectively, SPT - N_{cor} (*Equations 9*) and Modulus number (*Equation 10*).

$$c_u = q_{cn}/N_k \quad (3)$$

where C_u is unconfined compressive strength, N_k is equal to 17 to 18 for normally consolidated clays or 20 for over consolidated clay. The bearing capacity using normalized cone resistance values was determined for D/B ≤ 1.5 (in kg/cm^2):

$$Strip: Qult = 2 + 0.28q_c \quad (4)$$

$$Square: Qult = 5 + 0.34q_c \quad (5)$$

$$Q_{ult} = Q_{cn}/40 \; in \; kg/cm^2 \quad (6)$$

$$E_{strip} = 3.5 \times Q_{ult} \quad (7)$$

$$E_{square} = 2.5 \times Q_{ult} \quad (8)$$

$$N_{cor} = \frac{Q_c}{4} \quad (9)$$

$$Modulus\ Number = 22.4CBR^{0.5} \quad (10)$$

From the analysis, the followings were derived: settlement (both elastic and consolidation), activity (*Equation 9*), Group Index (GI), AASHTO and USCS classifications, suitability index (*Equation 10*), bearing pressure models were developed from CPT results using Hatanaka and Uchida (1996), Meyerhof (1956) and Schmertmann (1975) equations; with corresponding stresses (mean, +ve, and –ve stresses) using Burland and Burbidge (1984) model. Correlations were made between parameters: MDD/PI vs. CBR, LL vs. coefficient of consolidation, PI vs. undrained shear strength/effective overburden, PI vs. angle of shearing, dry density vs. angle of

shearing, suitability index vs. CBR, clay contents vs. PI. Mineralogy and micro fabric of the clay structure are studied using X-ray diffraction, differential thermal analysis and scanning electron microscope. In this study, the geochemical analysis was done using X-ray diffraction.

$$A = \frac{PI}{\%\ finer\ than\ 2.0\ mm} \tag{11}$$

$$Si = \frac{\%\ finer\ than\ 2.0\ mm}{LL \log(PI)} \tag{12}$$

The acquisition of VES data was in line with Falowo and Dahunsi (2020) and Falowo and Olabisi (2020) using Schlumberger array with maximum current – current spread of 130 m, and potential – potential distance of 5 m. A total of thirty-one VES were acquired. The quantitative interpretation of the VES curves involved partial curve matching and computer iteration technique. This technique assumes that the earth is made up of horizontal layers with differing resistivities. Any significant deviation (in dip angle greater than 10%) from this planar assumption in the stratigraphy will slightly distort the VES curve and introduce error in the VES interpretation results. Other sources of error are lateral inhomogeneity, suppression, and equivalence. All these were taken care of during data analysis and interpretation. The depth sounding interpretation is presented as geoelectric section, which showed horizontal to near horizontal stratification of subsurface geologic layers.

Magnetic method was also used, with measurements taken at 1 m interval along a traverse with GSN 8 Proton Precision Magnetometer. The field procedures were in line with Falowo et al. (2015). The distance covered for the survey was 500 m, using the same traverse established for the VES. Two sets of data were collected at each location and average determined, with sensor height at 1.5 m. The base station readings were taken before and after the data acquisition.

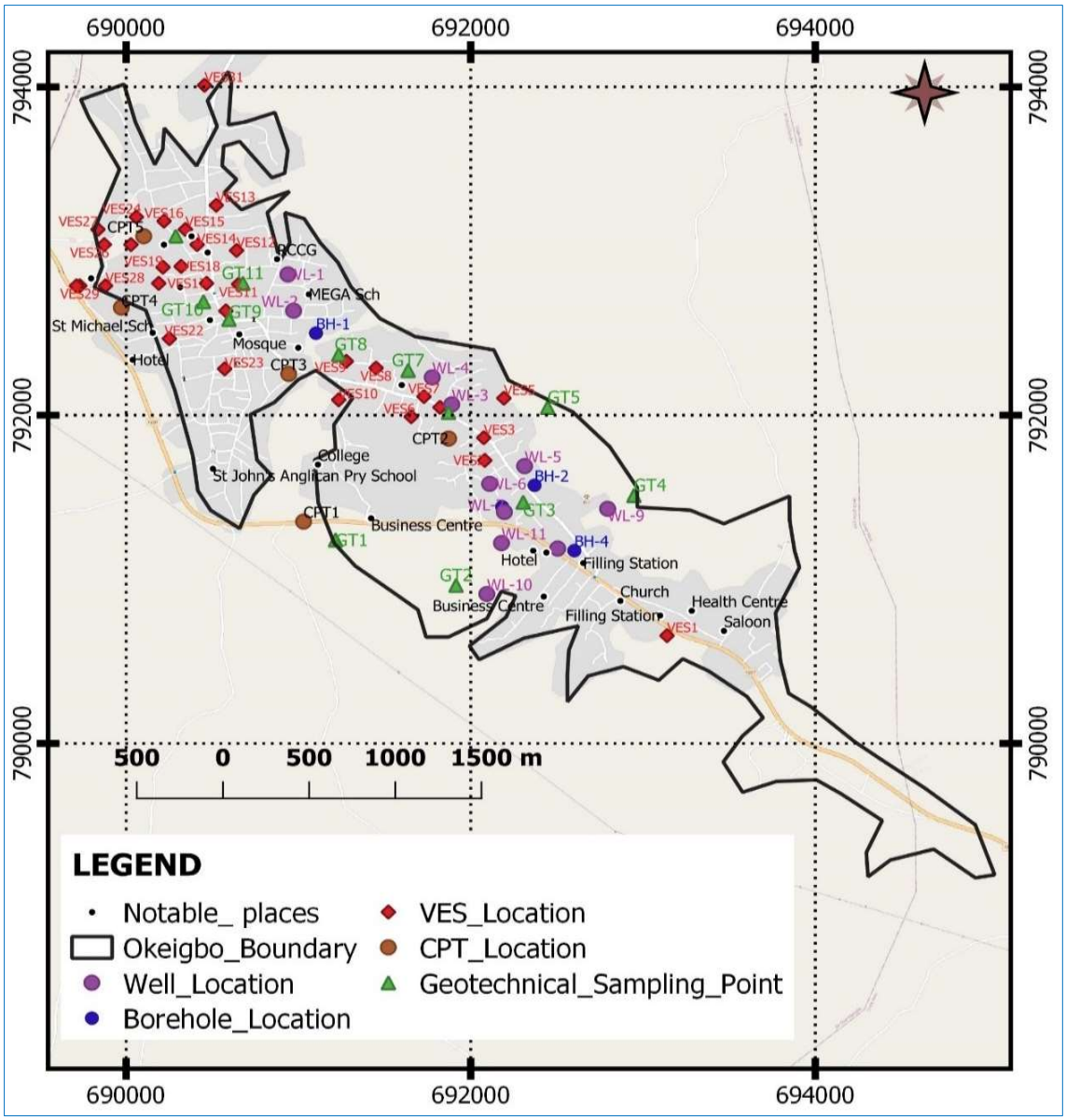

Fig. 5. Data Acquisition map showing the field surveys and laboratory sampling points

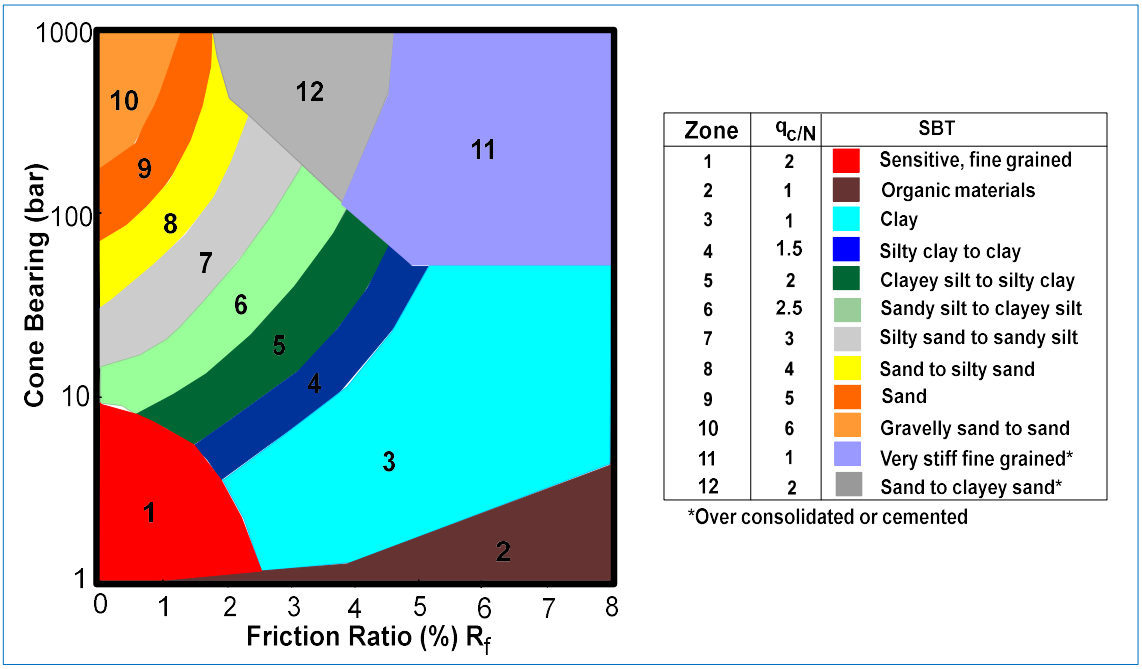

Fig. 6. Robertson Chart for Soil Classification using Cone Resistance Value and Friction Ratio (Robertson, 1990)

The base station reading was used to correct the data for diurnal and offset corrections. The scope of engineering site investigation must be extended if the water (groundwater) is known or suspected that the ground in question has been contaminated by harmful substances such as organic or inorganic chemicals, fibrous materials such as asbestos, toxic or explosive gases, biological agents and radioactive elements. These contaminants influence all other aspects of ground investigation and may have consequences for foundation design and the general suitability of the site for intended purposes. These features were not reported in the water samples from desk study/literature review. In addition, personal interviews with inhabitants of the town responded negatively to aforementioned elements.

Consequently, no water quality test was carried out. However, the static water level, hydraulic head determination, and hydraulic conductivity was done using eleven open wells (Brassington, 1988). The number of wells was limited due to reliance by the town on government boreholes and streams.

3. Results and Discussion

3.1. Geology

The major geological units observed (as outcrops) in the area are quartz schist and quartzite which is flaggy, (Fig. 7). In many places, quartzite is found in association with quartz schist, and is concealed by a variable thick overburden which in many places are clayey or laterite. This soil material (Fig. 8) is being excavated and transported to construction sites for different forms of projects such as highway construction, embankment, and fillings.

The observed quartzite occurred as boulders, elongated ridges and weathered rock; has fine texture and non-foliated, formed by both contact and dynamic metamorphism or from cementation of silica. It is very strong and durable, with the principal mineral being quartz. The colour of the quartzite varied across the study as white, pink, yellow or gray tints, depending on its impurities. The observed mineralogy consists of quartz, with zircon, hematite, tourmaline, muscovite, staurolite, graphite, sillimanite as minor minerals. Structural features such as joints and fractures were observed, and in many places are filled with laterite or clayey sand. Subsequently, quartzite is hard, compact, thoroughly crystalline are very strong, therefore can afford good ground condition. However, caution has to be exercised in areas where they are intensely weathered and/or showed prominent fracture and joint system.

The Schist on the other hand is megascopically crystalline foliated metamorphic rocks characterized by a typical schistose structure (Attewell and Farmer, 1988). The constituent flaky and platy minerals are mostly arranged as parallel or sub parallel layers or bands. They are characterized by textures with marked preferred orientation. These preferred alignment of platy minerals accounts for their schistocity. They appear appreciably stronger across than along the mineral lineation. It is medium to coarse in texture and foliated with schistose structure. It contains readily visible slaty cleavages. Mica and chlorite are common minerals, with feldspar in lesser amounts; quartz and feldspar are comparatively rare or minute. Not only do those cleavage and schistocity adversely affect the strength of schist, but it also makes them susceptible to decay. In fact, schist weather slows but could undergo extensive regional metamorphism resulting in folding, fracture. Consequently, they are variable in quality, some being excellent foundation for heavy structures, others regardless of the degree of their deformation and weathering are so poor. Some schists become slippery on weathering and therefore fail under a moderately light load.

Falowo (2019) conducted geotechnical analysis of some rocks (porphyritic granite, fine grained granite, migmatite, granite gneiss, quartz schist, granodiorite, charnockite, and quartzite) within the same geological province, for aggregate impact value, aggregate crushed value, point load strength test, specific gravity, water absorption and unconfined compression test, and direct shear strength using BS, ASTM D-2216 and ISRM procedures. These rocks are supposed to be contemporaneous with those in the study area, as they both displaced the same structural features in magnitude and direction. The Aggregate Impact Value (AIV) recorded 11.2 (quartzite) and 12.4 (quartz schist); Aggregate crushed value (ACV) 18.4 (quartzite) and 22.2 (quartz schist), and unconfined compressive strength (UCS) 159.4 MPa (quartz schist) and 185.3 MPa (quartzite); point load strength index (PLSI) 8.84 MPa (quartzite) and 8.89 (quartz schist); and shear strength of 79.7 MPa (quartz schist) and 92.6 MPa (quartzite). Therefore, quartzite shows more quality than schist, thus will be useful material for foundation constructions, aggregate in pavement, building stone, and armourstones (Smith and Collis, 2001; Archana and Kumar, 2016).

The compressive strength of a rock depends on a number of factors such as mode of formation, composition, texture, structure, moisture content, and extent of weathering. According to Hunt (2005) metamorphic rock has been crystalline in character, compact, and interlocking in texture and uniform in structure, and possess very high compressive/shear strength, modulus of elasticity. However, the degree of its foliation, schistocity, and cleavage greatly affect their compressive strength in magnitude and direction.

Table 1 showed that the residual soils of most metamorphic rocks are low activity clays and granular soil, which is in agreement with earlier results, while Table 2 showed the expected properties of rocks observed in the study area, as they are expected to have very high strength, low deformability; and presumable bearing capacity of 4, 000 – 12, 000 KPa (Table 3) especially when fresh (FR), and in between 2500 – 8000 KPa when partly or slightly weathered (SW).

3.2. VES Technique

The summary of the VES is presented in Table 4, while a typical geologic section prepared for VESs 2, 6, 10, 22, 23, and 28, in SE – NW trend, is shown in Fig. 9. The curve types obtained from the study area varied from three-layer curves (H), four-layer curves (KH, HK, and QH), and five-layer curves (HKH and KHK). The H curve type is the most preponderant (34 %) followed by KH (24 %), HKH (22 %), QH (14 %), and KHKH (6 %). This implies that the area is generally made of high resistive topsoil, underlain by high conductive weathered layer, and basement rock.

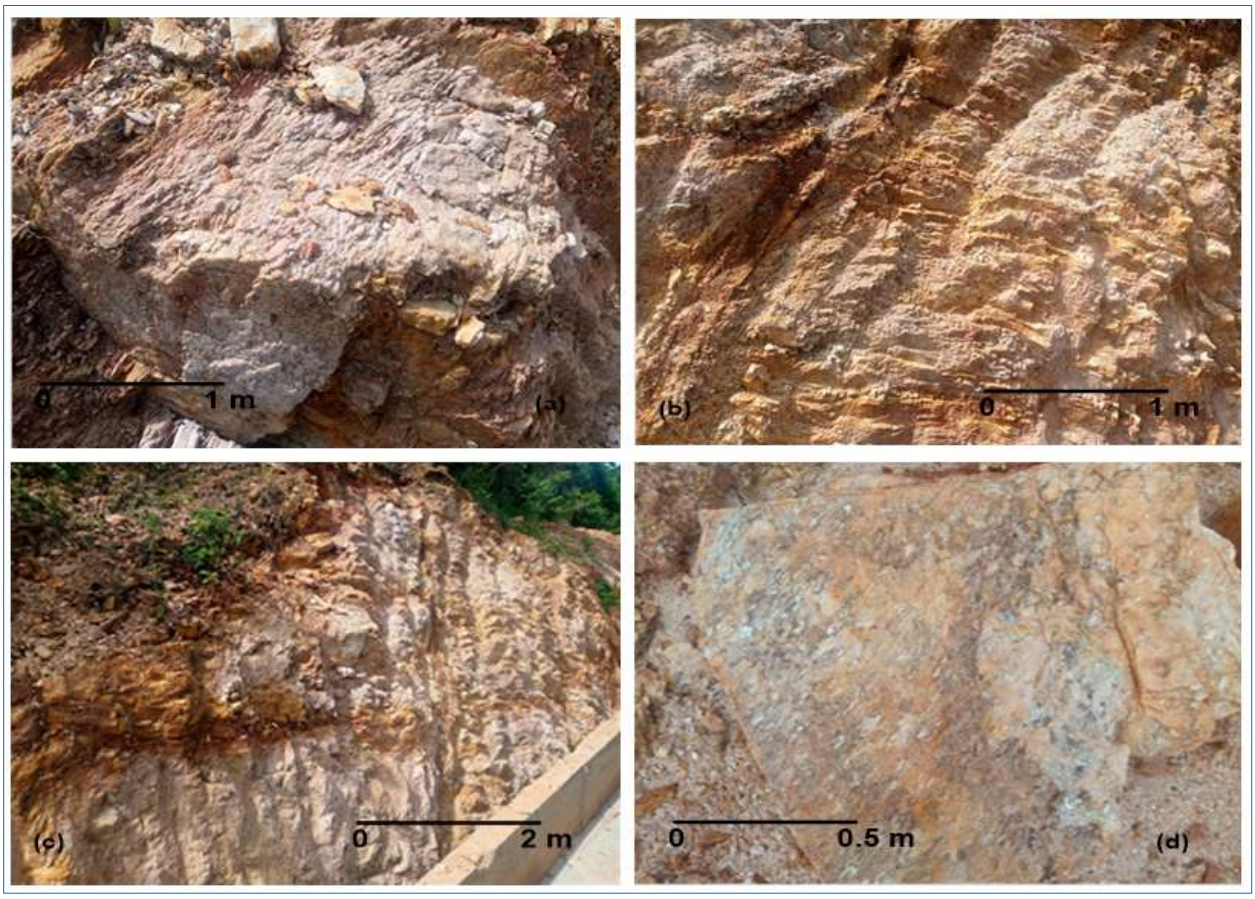

Fig. 7. Exposures of (a) – (c) Quartz schist displaying slaty cleavages, and had been affected by intense weathering, as they split along the plane of weakness (d) Schistose quartzite, and the less resistant minerals have been eroded leaving the more resistant minerals such as quartz and feldspar

Fig. 8. Exposures of (a) – (c) thick deposit of laterite and sandy clay at different locations within the study area (d-f) weathered rock material, with some occurring as boulders

Table 1. Classification of residual soils by its primary origin (Hunt, 2005)

Primary occurrence	Secondary occurrence	Typical residual soils
Granite	Saprolite	Low activity clays and granular soils
Diorite		
Gabroo	Saprolite	High activity clays
Basalt		
Dolerite		
Gneiss	Saprolite	Low activity clays and granular soils
Schist		
Phyllite		Very soft rock
Sandstone		The thin cover depends on impurities. Older sandstones would have thicker cover
Shales	Red, Black, marine	Thin clayey cover Friable and weak mass high activity clays
Carbonates	Pure Impure	No soil, rock dissolves Low to high activity clays

Table 2. General engineering properties of common rocks (Hunt, 2005)

Rock origin	Type	Characteristics	Permeability	: Deformability	Strength
Igneous coarse to medium grained – very slow to slow cooling	Granite, granodiorite, diorite, peridiorite	Welded interlocking grains, very little pore space	Essentially impermeable	Very low	Very high
Igneous fine grained – rapid cooling	Rhyolite, trachyte, quartz, dacite, andesite, basalt	Similar to above or can contain voids	With voids can be highly permeable	Very low to low	Very high to high
Igneous glassy – very rapid chilling	Pumice, scoria, vesicular basalt	Very high void ratio	Very high	Relatively low	Relatively low
Sedimentary – arenaceous clastic	Sandstones	Voids cement filled. Partial filling of voids by cement coatings	Low Very high	Low Moderate to high	High Moderate to low
Sedimentary – argillaceous clastic	Shales	Depends on degree of lithification	Impermeable	High to low, can be highly expansive	Low to high
Sedimentary – arenaceous clastic chemically formed	Limestone	Pure varieties normally develop caverns	High through caverns	Low except for cavern arch	High except for cavern arch
Metamorphic	Gneiss	Weakly foliated	Essentially impermeable	Low	High
		Strongly foliated	Very low	Moderate normal to foliations. Low parallel to foliations	High- normal to foliations. Low parallel to foliations
Metamorphic	Schist	Strongly foliated	Low	As for gneiss	
Metamorphic	Phyllite	Highly foliated	Low	Weaker than gneiss	
Metamorphic	Quartzite	Strongly welded grains	Impermeable	Very low	Very high
Metamorphic	Marble	Strongly welded	Impermeable	Very low	Very high

From Table 1, topsoil has resistivity ranging from 36 – 2363 ohm-m (avg. 255 ohm-m) and thickness varying from 0.7 – 4.9 m (avg. 1.55 m) and composed of clay, sandy clay, clayey sand, sand, and laterite. The subsoil is characterized with resistivity ranging from 96 – 3561 ohm-m (avg. 1149 ohm-m) and have same composition as the topsoil, with thickness ranging from 1.5 to 15.8 m (avg. 5.68 m). The weathered layer has resistivity ranging between 38 ohm-m and 1202 ohm-m (avg. 240 ohm-m), indicating clayey weathered layer; the thickness ranged from 4.2 m and 25.5 m (avg. 14.1 m). The fractured basement was delineated under VES 4, and has resistivity of 226 ohm-m with thickness of 8.3 m. The depths to basement rock varied from 8.2 – 31.5 m (avg. 20.9 m), indicating moderate/thick weathering profile, and resistivity ranging from 258 – 4520 ohm-m (avg. 2035 ohm-m). Consequently, the topsoil, subsoil, and weathered layer are generally composed of sandy clay and laterite material, which can be regarded fair/good soil material to support the civil engineering structures, depending on the intended use. Typical sections shown in Fig. 7 are characterized by topsoil (55 – 2363 ohm-m), subsoil (374 – 1327 ohm-m), weathered layer (66 – 350 ohm-m), fractured basement (258 – 854 ohm-m) and basement rock (1876 – 2303 ohm-m). The relief of the basement is rugged.

Table 3. Estimate of allowable bearing capacity in rock (Hunt, 2005)

Materials	Presumed allowable bearing capacity (kPa)			
	XW	DW	SW	FR
Igneous				
Tuff	500	1,000	3,000	5,000
Rhyolite, Andesite, Basalt	800	2,000	4,000	8,000
Granite, Diorite	1,000	3,000	7,000	10,000
Metamorphic				
Schist, Phyllite, Slate	400	1,000	2,500	4,000
Gneiss, Migmatite	800	2,500	5,000	8,000
Marble, Hornfels, Quartzite	1,200	4,000	8,000	12,000
Sedimentary				
Shale, Mudstone, Siltstone	400	800	1,500	3,000
Limestone, Coral	600	1,000	2,000	4,000
Sandstone, Greywacke, Argillite	800	1,500	3,000	6,000
Conglomerate, Breccia	1,200	2,000	4,000	8,000

Table 4. Interpreted VES results

East	North	Elevation (m)	VES No	Resistivity (Ohmns-meter)					Thickness (m)				Depth (m)				Curve Type
				ρ_1	ρ_2	ρ_3	ρ_4	ρ_5	h_1	h_2	h_3	h_4	d_1	d_2	d_3	d_4	
693140	790657	228	1	188	312	1332			1.9	14.2			1.9	16.1			H
692082	791725	247	2	222	96	854	258		0.8	3.2	4.2		0.8	4	8.2		HK
692076	791863	245	3	55	290	102	2111		1.8	1.5	10.2		1.8	3.3	13.5		KH
691822	792048	231	4	350	185	1875	226	3255	1.1	2.9	8.3	13.9	1.1	4	12.3	26.2	HKH
692193	792104	241	5	186	843	302	2259		1.1	3.6	19.7		1.1	4.7	24.4		KH
691655	791991	227	6	159	374	86	668		1.9	2.4	8.9		1.9	4.3	13.2		KH
691729	792114	227	7	303	999	55	1113		2.3	9.6	12.3		2.3	11.9	24.2		KH
691451	792288	218	8	405	991	112	2531		0.9	8.6	17.8		0.9	9.5	27.3		KH
691278	792329	212	9	224	2587	47	1236		1.6	3.8	15.3		1.6	5.4	20.7		KH
691234	792094	213	10	2363	1212	66	2303		2.5	8.7	16.3		2.5	11.2	27.5		QH
690653	792799	224	11	195	2637	126	3303		4.6	3.9	12.2		4.6	8.5	20.7		KH
690641	793004	220	12	147	3561	144	3362		4.9	3.8	19.9		4.9	8.7	28.6		KH
690523	793280	217	13	151	1005	38	3652		1.2	7.9	8.2		1.2	9.1	17.3		KH
690412	793040	234	14	158	1488	265	2105		1.9	7.4	9.7		1.9	9.3	19		KH
690344	793132	237	15	89	1145	69	3647		1.1	6.7	14.1		1.1	7.8	21.9		KH
690220	793183	240	16	155	1063	88	899		1.2	3.9	19.3		1.2	5.1	24.4		KH
690467	792804	235	17	78	277	95	2212		1.1	9.3	13.4		1.1	10.4	23.8		KH
690319	792907	243	18	389	784	111	2197		0.9	1.5	25.5		0.9	2.4	27.9		KH
690214	792902	243	19	80	1176	78	4520		1.6	8.8	19.8		1.6	10.4	30.2		KH
690189	792804	247	20	408	878	123	2998		0.8	15.3	15.4		0.8	16.1	31.5		KH
690579	792636	235	21	83	654	101	1222		0.7	2.4	9.9		0.7	3.1	13		KH
690251	792467	265	22	55	325	85	665		0.8	7.4	20.5		0.8	8.2	28.7		KH
690572	792283	244	23	265	989	94	3017		1.2	2.9	18.4		1.2	4.1	22.5		KH
690059	793208	230	24	175	1202	323			1.9	12.3			1.9	14.2			K
690028	793040	224	25	37	1032	258	2141		0.9	3.4	9.9		0.9	4.3	14.2		KH
689873	793040	200	26	187	3117	285	888		1.9	2.2	14.8		1.9	4.1	18.9		KH
689836	793132	197	27	225	523	287	1743		1.5	2.8	16.6		1.5	4.3	20.9		KH
689880	792789	223	28	220	1327	350	1876		1.1	5.5	22.7		1.1	6.6	29.3		KH
689731	792789	215	29	211	458	1456			1.2	8.9			1.2	10.1			A
689712	792789	214	30	36	365	622	1478		0.8	6.5	11.2		0.8	7.3	18.5		AA
690455	794011	211	31	102	448	2322			0.9	10.4			0.8	11.2			A

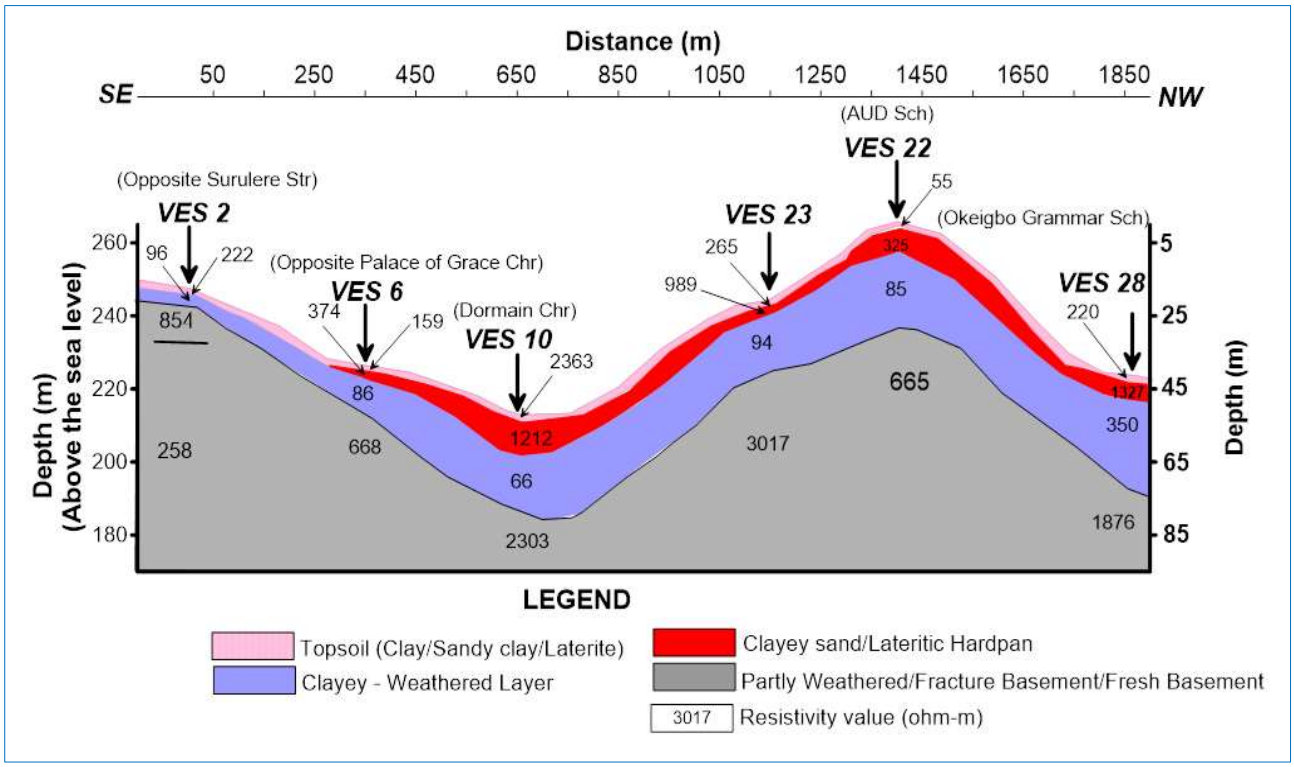

Fig. 9. Geologic section/profile along the selected VES point established in the study area

The spatial distribution map of weathered layer resistivity, thickness, overburden thickness, and traverse resistance are shown in Fig. 10. The weathered layer resistivity in Fig. 10a showed values generally less than 150 ohm-m especially in the central part, while values in the range of 150–250 ohm-m are common in the northern and southern areas; with highest thickness of 17.4 – 24.2 m map found in the central part (Fig. 10b).

The overburden thickness in the range of 22–31 m is the most dominant (Fig. 9c), and transverse resistance in the range of 5000–8500 ohm-m^2 and 8500 - 11500 ohm-m^2 (Fig. 10d) characterized the southern and central zone respectively. Consequently, the central part showed more competence than other parts of the study.

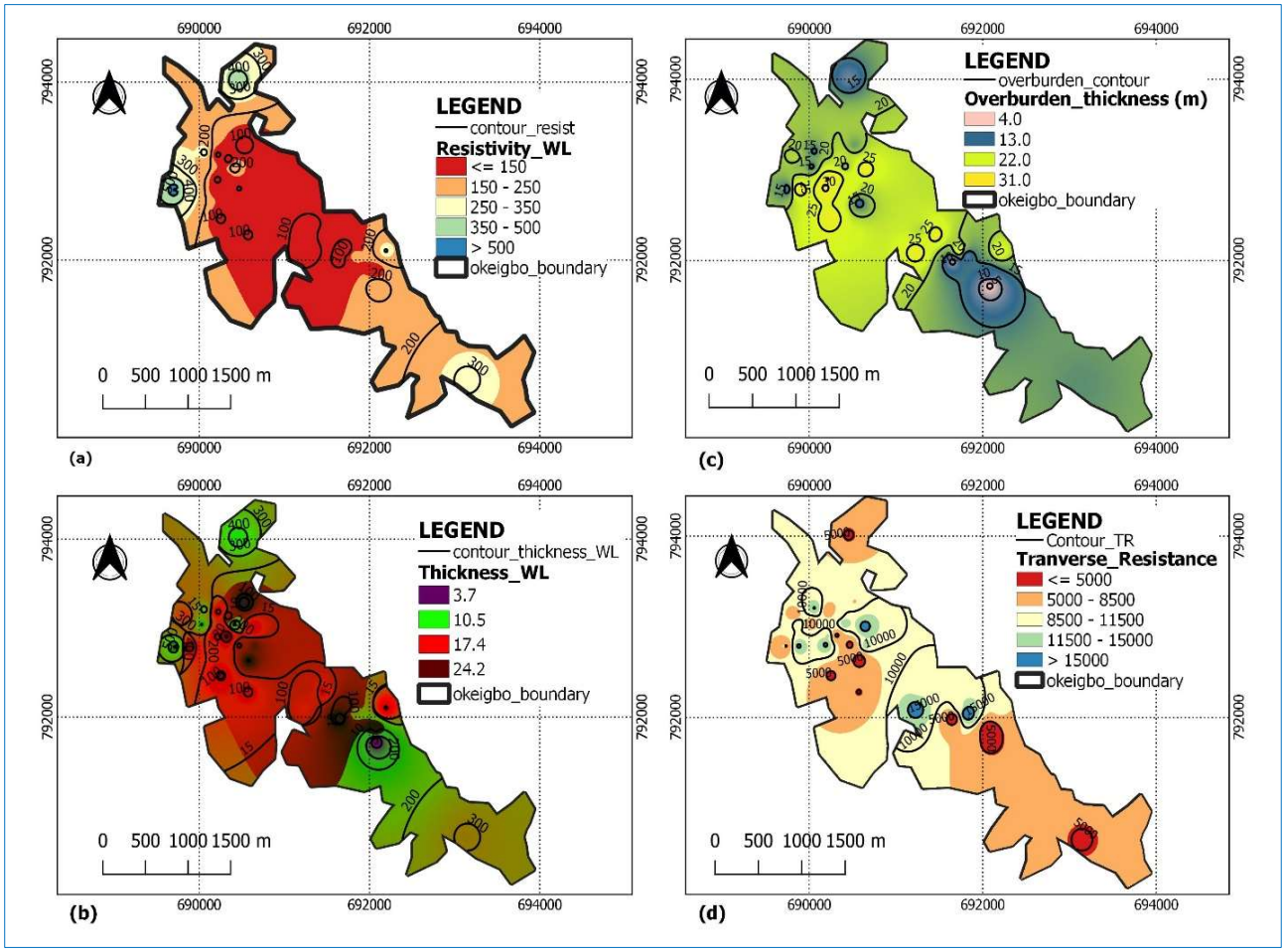

Fig. 10. Spatial distribution of (a) weathered layer resistivity (b) weathered layer thickness (c) overburden thickness (d) transverse resistance, across the study area

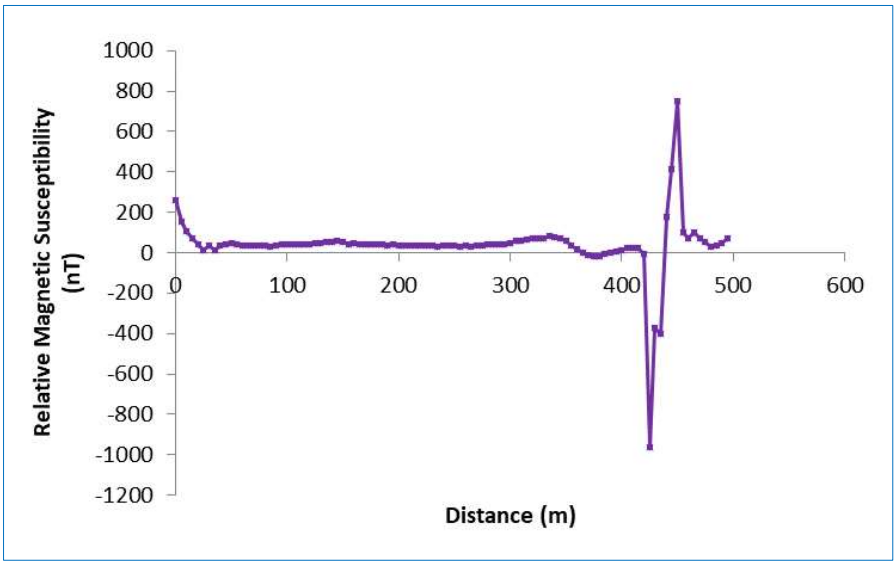

Fig. 11. Magnetic Profile along the selected VESs 2, 6, and 10

3.3. Magnetic Method

The relative magnetic field intensity along the profile (Fig. 11) covering VESs 2, 6, and 10, of total distance of 500 m in SE – NW trend showed amplitude variation of -964 nT to 748.75 nT (avg. 37.22 nT). This range of value is not unusual in basement complex, as similar values of -284 to 228 nT, -391 to 114 nT, -199 to 856 nT had been reported by Falowo et al. (2015).

The profile showed a relatively flat anomaly, which can be considered as magnetically homogeneous environment. However low and high magnetic anomalies observed as distances 420 – 460 m are indication of structural features such as fracture, lineation, fault or joint system i.e., for low amplitude; and possibly intrusion like sill, dyke for the abnormal high amplitude.

3.4. Borehole Sections

The geologic section observed from four borehole cuttings is shown in Fig. 12. The cuttings were visually inspected in their natural state or condition. The geologic units observed from the sites investigated and their depths range are clay/lateritic clay (2.5–7.5 m), sandy clay (2.5–15.5 m), clayey sand (3.0–27.5 m), clay-sand mixture (18.0–28.5 m) and basement rock 24.5 (quartz schist)–33.5 m (quartzite). The static water level ranged between 10.5–18.5 m. Consequently, the SWL is deep in the study area. However, the upper 10 m is composed of sandy clay, and clay/lateritic clay.

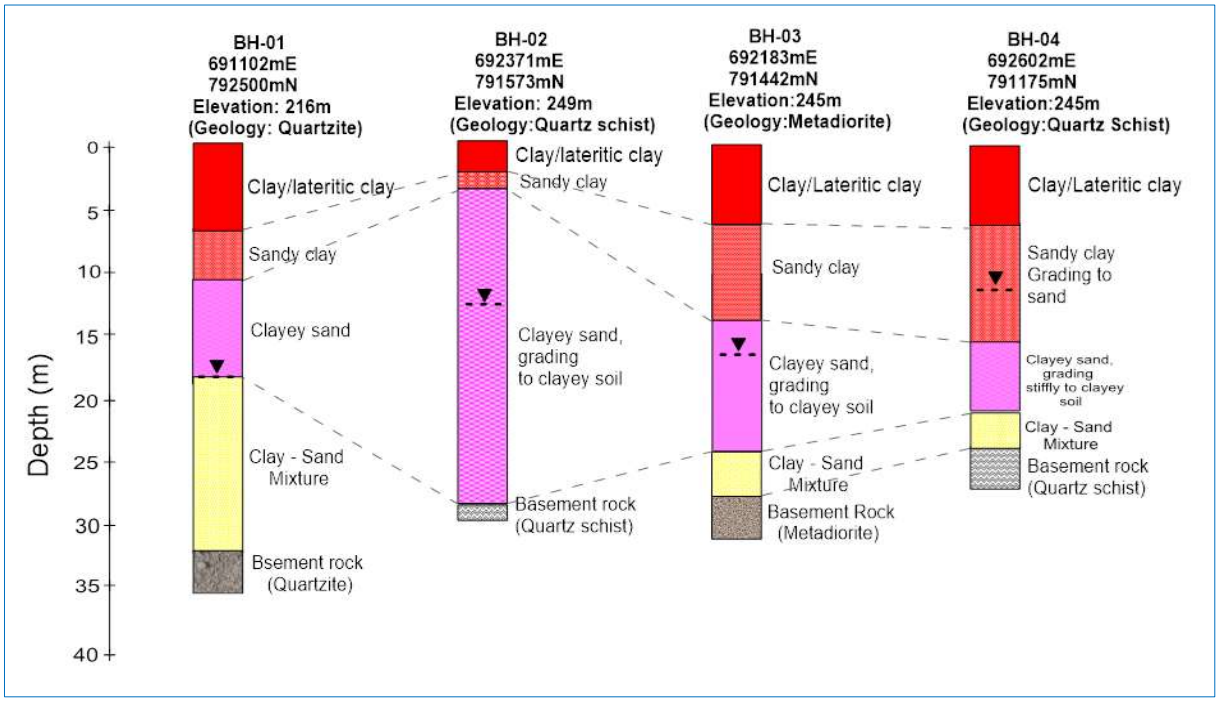

Fig. 12. Borehole sections showing the various geologic units observed from borehole cuttings

3.5. Hydrogeological Study

Hydrogeological investigation enables the prediction about the influence of groundwater system in civil engineering works. This can be carried out to assess location and thickness of water zone, their confinement, and hydrogeological margins; the levels of water and their variations with seasons (time); their storage potential and transmissivity; and their quality (Brassington, 1988).

The data acquired from fifty across different rocks is presented in Table 5. The total depth of the well investigated ranged from 5.2 (quartzite) – 10.1 m (quartzite) (avg. 7.5 m), even though the depth of the wells is at owner's discretion and availability of funds, but useful data were acquired.

The water column which is storage/reservoir potential of the wells ranged from 1.3 (quartzite)–4.8 m (metadiorite) (avg. 3.40 m). The SWL varied from 2.2 m to 6.5 m (4.1 m), with corresponding hydraulic head of 215.1–244.9 m above the seal level (avg. 233.21 m). The information from the boreholes in Table 6, with total depth ranging from 25 (quartz schist)–35 m (quartzite) and an average of 30 m, showed SWL ranging from 10–18 m (avg. 13.75 m).

3.6. Geochemical Analysis

The stability and serviceability performance of soil for construction works is contingent upon the mineralogical make-up of the soil (Bell, 2004; Bell, 2007).

The result of chemical analysis of selected mineral oxides contained in the soil samples, and silica-sesquioxide (S-S) ratio is presented in Table 7. They ranged from: MgO (0.09-0.45 %, avg. 0.28%), Al_2O_3 (16.47–18.35 %, avg. 17.20 %), SiO_2 (50.22–61.50 %, avg. 54.91 %), P_2O_5 (0.01–0.12 %, avg. 0.041 %), Na_2O (0.09–1.23 %, avg. 0.535 %), K_2O (0.32–2.12 %, avg. 0.77 %), CaO (0.08–0.72 %, avg. 0.25 %), TiO_2 (0.35–1.73 %, avg. 1.195 %), V_2O_5 (0.01–0.88 %, avg. 0.38 %), Cr_2O_3 (0.01–0.05 %, avg. 0.03 %), MnO (0.03–0.15 %, avg.

0.08 %), Fe_2O_3 (22.47–28.1 %, avg. 25.83 %), and CuO (0.01–0.25 %, avg. 0.06 %). Consequently, the soil is abundantly rich in SiO_2, Fe_2O_3, and Al_2O_3, with the concentration of SiO_2 more than combined concentrations of other mineral oxides. The S-S ratio varied between 1.13–1.55 (avg. 1.28). Accordingly, the soils' S-S ratio is within laterite/lateritic type range of less than <1.33 to 2.0 (Martin and Doyne, 1927).

Table 5. Summary of the well information obtained from Eleven wells across the wet and dry season

East	North	Well no	Elevation (m)	Total depth (m)	SWL (m)	Water column	Hydraulic head (m)	Geology
690939	792858	WL-1	219	5.2	3.9	1.3	215.1	Quartzite
690972	792637	WL-2	222	5.5	2.8	2.7	219.2	Quartz schist
691890	792066	WL-3	233	7.8	4.1	3.7	228.9	Metadiorite
691777	792231	WL-4	227	9.3	4.5	4.8	222.5	Metadiorite
692313	791690	WL-5	250	8.2	5.1	3.1	244.9	Quartzite
692110	791582	WL-6	246	5.9	2.2	3.7	243.8	Metadiorite
692196	791410	WL-7	245	8.5	3.9	4.6	241.1	Metadiorite
692505	791188	WL-8	246	10.1	6.5	3.6	239.5	Quartzite
692795	791430	WL-9	247	9.8	5.4	4.4	241.6	Quartz schist
692094	790911	WL-10	234	5.8	3.0	2.8	231	Quartz schist
692179	791221	WL-11	241	6.2	3.3	2.9	237.7	Quartz schist

Table 6. Borehole Information obtained from six boreholes

East	North	Borehole No	Elevation (m)	Total depth (m)	SWL (m)	Geology	Present state
691102	792500	BH-1	216	35	18	Quartzite	Functioning
692371	791573	BH-2	249	28	12	Quartz schist	Functioning
692183	791442	BH-3	245	32	15	Quartz metadiorite	Functioning
692602	791175	BH-4	245	25	10	Quartz schist	Functioning

Table 7. Result of the chemical analysis of selected mineral oxide

Sample No.	MgO	Al_2O_3	$Si0_2$	P_2O_5	Na_2O	K_2O	CaO	$Ti0_2$	V_2O_5	Cr_2O_3	MnO	Fe_2O_3	CuO	Sesquioxide Ratio	Class
OK-1	0.33	16.89	61.50	0.01	0.56	0.41	0.08	1.73	0.88	0.03	0.03	22.90	0.02	1.55	Lateritic
OK-2	0.29	16.80	50.30	0.01	1.23	0.32	0.10	1.19	0.08	0.03	0.13	26.85	0.02	1.15	Laterite
OK-3	0.24	18.35	51.65	0.11	0.63	0.38	0.23	0.98	0.09	0.05	0.15	27.20	0.02	1.13	Laterite
OK-4	0.20	16.50	52.20	0.01	0.61	0.44	0.23	0.35	0.11	0.03	0.05	25.60	0.01	1.24	Laterite
OK-5	0.42	16.80	51.68	0.02	0.65	1.54	0.72	1.24	0.03	0.03	0.12	27.84	0.11	1.16	Laterite
OK-6	0.28	16.55	60.22	0.08	0.23	0.48	0.28	1.21	0.07	0.05	0.13	25.68	0.25	1.43	Lateritic
OK-7	0.15	16.86	59.50	0.01	0.14	0.41	0.17	1.04	0.01	0.01	0.15	27.22	0.09	1.35	Lateritic
OK-8	0.45	18.20	55.21	0.12	0.16	2.12	0.32	1.52	0.09	0.02	0.05	28.10	0.02	1.19	Laterite
OK-9	0.09	17.65	54.30	0.07	0.09	0.85	0.15	1.32	0.81	0.03	0.03	22.47	0.02	1.35	Lateritic
OK-10	0.23	17.32	51.68	0.02	1.02	0.69	0.28	0.87	0.85	0.03	0.03	24.65	0.03	1.23	Laterite
OK-11	0.38	16.47	50.22	0.01	0.58	1.11	0.28	1.23	0.83	0.05	0.03	27.12	0.05	1.15	Laterite
OK-12	0.27	17.98	60.42	0.02	0.52	0.48	0.11	1.66	0.72	0.05	0.05	24.33	0.05	1.43	Lateritic

Table 8. Summary of geotechnical analysis showing the particle size distribution, consistency limit and soil classification

Sample No.	Location		Elevation (m)	NMC (%)	Grain size distribution				SG	Consistency Limits			SL	Group Index	AASHTO Class	USCS Class
	East	North			Sand (%)	Silt (%)	Clay (%)	Fines (%)		PL (%)	LL (%)	PI (%)				
OK-1	691216	791240	251	24.4	10.1	19.2	70.7	89.9	2.785	26.1	50.4	24.30	8.7	17	A-7-6	CH
OK-2	691915	790963	245	20.2	22.4	18.3	59.3	77.6	2.762	21.1	43.7	22.60	9.6	11	A-7-6	CL
OK-3	692305	791470	249	22.1	18.6	18.2	63.2	81.4	2.773	22.15	45.9	23.75	9.1	13	A-7-6	CL
OK-4	692948	791511	253	22.7	17.7	13.9	68.4	82.3	2.778	26.98	51.6	24.62	8.9	16	A-7-6	CH
OK-5	692447	792048	251	22.5	21.5	16.8	61.7	78.5	2.765	25.73	49.2	23.47	9.4	13	A-2-6	CL
OK-6	691872	792017	248	20.6	26.3	14.8	58.9	73.7	2.771	27.3	48.5	21.20	10.1	11	A-7-6	CL
OK-7	691637	792273	246	24.1	18.6	12.2	69.2	81.4	2.774	25.71	50.6	24.89	9.7	17	A-7-6	CL
OK-8	691234	792370	250	27.6	24.4	17.1	58.5	75.6	2.763	19.18	44.4	25.22	8.3	12	A-7-6	CL
OK-9	690597	792584	249	20.8	33.2	6.1	60.7	66.8	2.762	26.09	47.3	21.21	9.9	11	A-7-6	CL
OK-10	690449	792692	251	22.3	19.9	12.8	67.3	80.1	2.775	26.75	50.1	23.35	10.2	15	A-7-6	CH
OK-11	690678	792804	251	25.5	23.8	7.7	68.5	76.2	2.776	23.98	48.5	24.52	9.5	16	A-7-6	CL
OK-12	690288	793091	249	28.2	24.2	3.9	71.9	75.8	2.762	20.97	42.6	21.63	9.5	14	A-7-6	CL

Table 9. Summary of Geotechnical Analysis showing the grading curve properties, CBR, cohesion, and consolidation parameters

Sample No.	Unit weight (kN/m³)	Triaxial Test		UCS (kPa)	K (cm/s)	Clay mineralogy	Activity	
		Cohesion (kN/m²)	Angle of friction (°)				Values	Soil type
OK-1	16.32	70.3	10.4	185.9	2.76E-08	I-M	0.34	Inactive
OK-2	17.27	81.2	12.3	230.3	4.43E-08	I-M	0.38	Inactive
OK-3	17.19	79.3	11.5	220.2	3.58E-08	I-M	0.38	Inactive
OK-4	17.75	75.6	8.2	218.5	3.55E-08	I-M	0.36	Inactive
OK-5	18.52	70.9	8.4	191.3	4.12E-08	I-M	0.38	Inactive
OK-6	18.50	72.4	9.3	211.4	4.02E-08	K	0.36	Inactive
OK-7	17.85	79.8	7.5	219.6	3.58E-08	I-M	0.36	Inactive
OK-8	17.65	73.8	7.6	186.1	4.06E-08	I-M	0.43	Inactive
OK-9	18.23	79.9	8.1	220.2	3.15E-08	K	0.35	Inactive
OK-10	18.60	66.7	6.8	192.3	3.10E-08	K	0.35	Inactive
OK-11	17.75	76.2	8.9	206.8	3.98E-08	I-M	0.36	Inactive
OK-12	17.63	71.7	9.2	199.6	3.69E-08	I-M	0.30	Inactive

3.7. Geotechnical Analysis

Tables 8-10 present the summary of the geotechnical results. The natural moisture content varied from 20.2 to 28.2 % (avg. 23.42 %), this range is not within 5–15 % acceptable range favourable for civil engineering uses. The concepts of grading and plasticity, and the use of these properties to identify, classify and assess soils, are the oldest and most fundamental in soil mechanics. Grading is the distribution of sizes that make up a particular soil. Thus, grading of a soil determines many of its characteristics. Since it is such an obvious property, and easy to measure, it is plainly the first choice as the most fundamental property to assess the characteristics of soil particularly the coarse-grained soils where mineral composition is relatively important. Grain size analysis can be used to characterize the subsoil material for engineering works, which can serve as a guide to the engineering performance of the soil type and also provides a means by which soils can be identified quickly. The sand content ranged from 10.1–33.2 % (avg. 21.73 %), % silt and clay contents ranged from 3.9 to 19.2 % (avg. 13.42 %) and 58.5 to 71.9 % (avg. 64.86 %). The % fines ranged from 66.8 to 89.9 (avg. 78.3). The composition of the soil is dominated (in order of magnitude) by clay, sand, and silt. The amount of %fines recorded is more than 35 % specification of Nigerian federal ministry of works and housing (FMWH, 1997) engineering construction.

The plasticity chart (Fig. 13a) shows that the fines in the samples are dominated by clay of low plasticity/ compressibility with LL generally less than 50 %. All the soil samples plotted above the A-line. In terms of clay mineralogy, 75 % the soil samples are plotted within the range of illite and montmorillonite, and 25 % kaolinite clay mineralogy group (Fig. 13b).

Kaolinite consists basically of alternating layers of silica, gibbsite sheets also termed as 1:1 mineral. In between the basic layers, there is a hydrogen bond holding them together. Hydrogen bond is very strong, prevents hydration and allows the layers to stack up to make around 100 layers thick.

Montmorillonite is made up of two silica sheets and one gibbsite sheet and bonded by Vander wall forces between the tops of silica sheets is weak and there's negative charge deficiency, water and exchangeable ions can enter and separate the layers. Hence montmorillonite has a very strong attraction for water and swells on absorption of water. Illite has a similar structure similar to montmorillonite, however in illite the interlayers are bonded together with a potassium ion linkage, making it to have relatively less attraction for water. Hence, in the presence of water montmorillonite will swell more than illite and kaolinite. The activity ranged from 0.30 to 0.43 (avg. 0.36) signifying inactive clay type.

Table 10. Summary of geotechnical analysis showing the grading curve properties, CBR, cohesion, and consolidation

Sample No.	MDD Kg/m³	OMC	CBR (Soaked)	CBR (unsoaked)	C_v (m²/yr)	a_v MPa⁻¹	m_v MPa⁻¹	σ_p MPa	C_c Index	C_s	C_r	e_o
OK-1	1632	33.5	5	41	0.00882	0.61813	0.40831	0.0400	0.0808	0.00284	0.059	0.514
OK-2	1727	27.4	11	48	0.00940	0.50979	0.35596	0.0400	0.0668	0.00085	0.048	0.432
OK-3	1719	27.7	12	55	0.00966	0.48755	0.33646	0.0400	0.0639	0.00017	0.046	0.449
OK-4	1817	28.4	3	37	0.00971	0.62344	0.42320	0.0400	0.0744	0.00198	0.061	0.551
OK-5	1768	28.6	5	35	0.00992	0.62845	0.39985	0.0400	0.0528	0.00214	0.058	0.498
OK-6	1763	27.1	4	42	0.00984	0.60065	0.42122	0.0400	0.0465	0.00225	0.062	0.520
OK-7	1751	25.6	3	35	0.00963	0.53741	0.40363	0.0400	0.0654	0.00187	0.065	0.513
OK-8	1729	28.6	3	38	0.00979	0.56540	0.40754	0.0400	0.0966	0.00199	0.063	0.476
OK-9	1809	30.7	6	43	0.00971	0.48792	0.44574	0.0400	0.0572	0.00298	0.049	0.488
OK-10	1725	32.3	5	42	0.00989	0.62123	0.39859	0.0400	0.6091	0.00275	0.058	0.500
OK-11	1714	27.8	4	45	0.00960	0.55987	0.61248	0.0400	0.0655	0.00301	0.061	0.435
OK-12	1732	29.9	3	38	0.00977	0.61118	0.41180	0.0400	0.0934	0.00199	0.058	0.448

C_v - coefficient of consolidation a_v - Coefficient of compressibility m_v - Coefficient of Vol. compressibility σ_p - Preconsolidation pressure C_c - Compression index C_s - Swelling index C_r - Recompression index

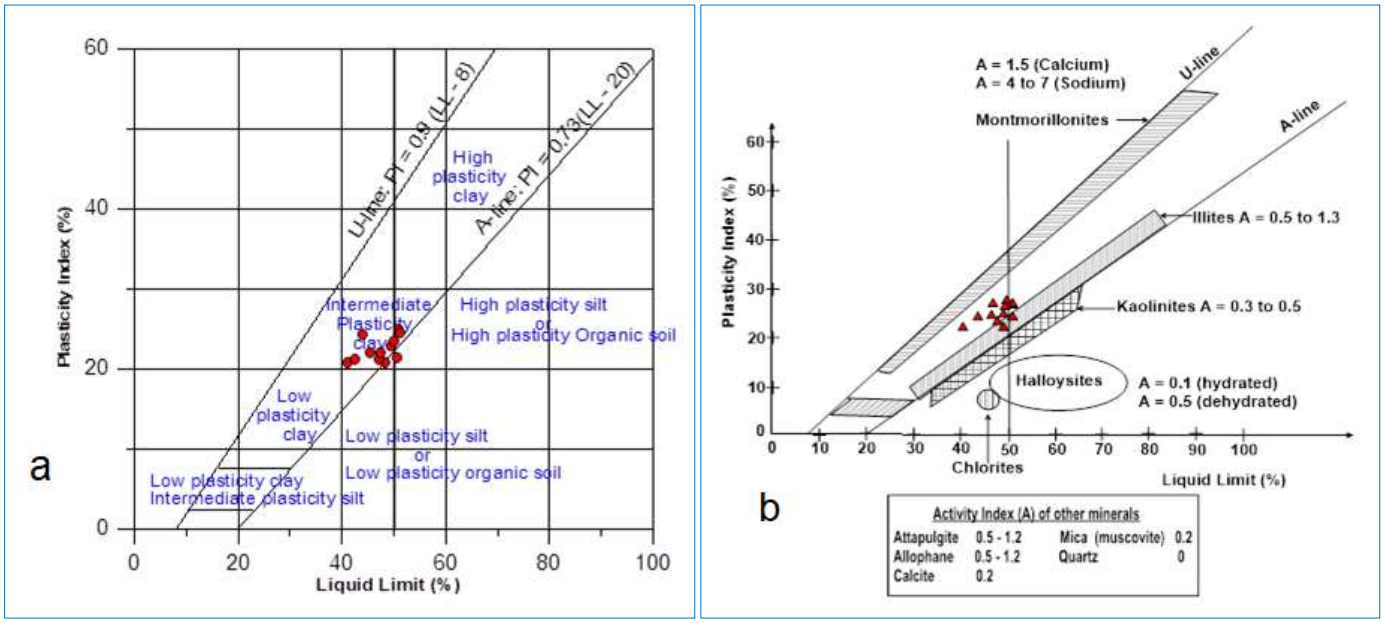

Fig. 13. (a) Plasticity chart for fine contents of the soil samples (b) Clay mineralogy group of the soil samples with most within illite – illite/montmorillonite

The specific gravity (SG) is closely related with soil's mineralogy and/or chemical contents; the higher SG, the higher the degree of laterization. In addition, the larger the clay fraction and alumina contents, the lower is the SG. The values of specific gravity of the samples ranged between 2.762–2.785 (avg. 2.771). The standard range of value of specific gravity of soils lies between 2.60 and 2.80, these values are considered normal for construction works; using the average value of 2.77, the soils fall within the inorganic clay/soils with mica or iron.

The liquid limit (LL) values ranged between 42.6 to 51.6 % (avg. 47.7 %), plastic limits (PL) ranged between 19.18 to 27.3 % (avg. 24.34 %) and plasticity index (PI) is between 21.2 to 25.22 % (avg. 23.40 %). Soil with high LL, PL, and PI are usually characterized with low bearing pressure. Hence the soil does not satisfy these requirements as construction material, since PI is above 20 %. The linear shrinkage ranged between 8.3 to 10.2 % (avg. 9.4 %), signifying a medium swelling potential. The group index (GI) values obtained ranged from 11 to 17 (avg. 14) corresponding to poor subgrade soil. The unit weight of the soils varied from 16.32–18.6 kN/m^3) (17.77 kN/m^3), cohesion of 66.7–81.2 kN/m^2 (avg. 74.81 kN/m^2), and angle of friction of 6.8–12.3° (avg. 9.0°).

The unconfined compressive strength (UCS) ranged from 185.9–230.3 kN/m^2 (avg. 206.9 kN/m^2). The hydraulic conductivity of the samples is between 2.76E-08 to 4.43E-08 cm/s (avg. 3.67E-08 cm/s) indicative of homogeneous, intact clays of practically impervious drainage condition as per BIS. The maximum dry density (MDD) for the soil samples varied between 1632 and 1817 kg/m^3 (avg. 1741 kg/m^3) at standard proctor compaction energy while the optimum moisture content (OMC) ranged between 25.6 and 33.5 % (avg. 29.0 %). All the soil samples have moderately high MDD at high OMC typical of clay soils. The California Bearing Ratio (CBR) is an empirical test employed in road engineering as an index of compacted material strength and rigidity, corresponding to a defined level of compaction (Upadhyay, 2015).

All compacted samples show soaked and un-soaked CBR values ranging between 3 and 12 % (avg. 5 %) and 35 – 55 % (avg. 42 %) respectively. These values are below the standard 10 % and 80 % standard for soaked and unsoaked CBR respectively for pavement subgrade construction. The consolidation characteristics of the soils showed coefficient of consolidation-C_v (0.00882–0.00992 m^2/yr; avg. 0.009645 m^2/yr), coefficient of compressibility-a_v (0.48755–0.62845 MPa^{-1}; avg. 0.570918 MPa^{-1}), coefficient of volume compressibility-M_v (0.33646–0.61248 m^2/kN; avg. 0.418732 m^2/kN), compression index-C_C (0.0465–0.6091; avg. 0.1144), swelling index-C_S (0.00017 to 0.00301; avg. 0.0021), recompression index-C_r (0.046–0.065; avg. 0.05733) and void ratio-e_o (0.432–0.551; avg. 0.4853). The preconsolidation pressure applied was 0.040 MPa.

Consequently, using the averages of all the consolidation parameters, based on C_c the soils are plastic clays (1.0–0.15) within medium compressibility i.e., 0.15 - 0.075; based on M_v the soils correspond to hard clay (0.125–0.625 m^2/kN). The coefficient of consolidation is indicative of the combined effect of compressibility and permeability of soil on the rate of volume change (Upadhyay, 2015).

3.8. CPT Analysis

The result of the CPT is presented in Table 11, while the plotted sounding curves for the eight locations is shown in Fig. 14 showing the cone resistance (Q_c), sleeve resistance (S_r), friction ratio (F_R), allowable bearing capacity, and Modulus Number (M-number) with depth. The obtained values of Q_c ranged from 28–138 kg/cm^2 (avg. 65 kg/cm^2), S_r varied from 46–675 kg/cm^2 (avg. 268 kg/cm^2), Q_{cn} is between

28 - 386 kg/cm^2 (avg. 177 kg/cm^2), F_R ranged from 2.85–4.89 (avg. 4.22), Q_{all} varied from 22.87–315.56 KN/m^2 (avg. 144.77 kN/m^2), UCS is in between 4.0–58.0 KN/m^2 (avg. 26.1 kN/m^2), C_u ranged from 2–29 KN/m^2 (avg. 13.1 kN/m^2), M-number varied from 6–78 (avg. 36), E_{square} is between 171.5–2369 kN/m^2 (avg. 1086 kN/m^2), E_{strip} ranged from 240–3313 kN/m^2 (avg. 1520 kN/m^2), N_{cor} varied from 3–35 (avg. 16), and σ_o is between 4.08–37.0 KN/m^2 (avg. 16.88 kN/m^2). The allowable bearing pressure for strip (Q_{strip}) and square (Q_{square}) ranged from 321–3600 KN/m^2 (avg. 686.7 kN/m^2), and 474 - 4455 KN/m^2 (avg. 2132.2 kN/m^2), respectively.

Table 11. Results of the CPT and other estimated soil properties using the resistance values

Depth (m)	Qc (Kg/cm^2)	Sr (Kg/cm^2)	Qcn (Kg/cm^2)	F_R	Qall (KN/m^2)	UCS (KN/m^2)	Cu (KN/m^2)	M-number	Esq (KN/m^2)	Estrip (KN/m^2)	N_{Cor}	σ_o (KN/m^2)	Qa Strip	Qa Square
CPT-1: 691030mE; 791352mN; 249m absl														
0.25	10	46	28	4.56	22.87	4.03	2.02	6	171.50	240	3	4.08	321	474
0.5	28	126	78	4.51	64.03	11.50	5.75	16	480.20	672	7	8.16	782	1034
0.75	35	163	98	4.67	80.03	14.24	7.12	20	600.25	840	9	12.24	962	1252
1.0	42	205	118	4.88	96.04	16.99	8.49	24	720.30	1008	11	16.32	1141	1469
1.25	60	255	168	4.25	137.20	24.29	12.15	34	1029.00	1441	15	22.90	1602	2029
1.50	75	299	188	3.98	153.13	26.99	13.50	38	1148.44	1608	19	27.48	1780	2246
1.75	88	322	220	3.66	179.67	31.66	15.83	44	1347.50	1887	22	32.38	2078	2607
2.0	118	486	283	4.12	231.28	41.05	20.53	57	1734.60	2428	30	37.00	2656	3309
CPT-2: 691872mE; 791858mN; 251m absl														
0.25	10	47	28	4.68	22.87	4.00	2.00	6	171.50	240	3	4.63	321	474
0.5	45	185	126	4.10	102.90	18.72	9.36	25	771.75	1080	11	9.26	1218	1563
0.75	68	243	190	3.57	155.49	28.29	14.14	38	1166.20	1633	17	13.89	1807	2278
1.0	75	299	210	3.98	171.50	31.00	15.50	42	1286.25	1801	19	18.52	1986	2496
1.25	98	343	274	3.50	224.09	40.54	20.27	55	1680.70	2353	25	23.56	2575	3211
1.50	118	422	319	3.58	260.19	47.02	23.51	64	1951.43	2732	30	28.28	2979	3702
CPT-3: 690944mE; 792252mN; 250m absl														
0.25	12	59	34	4.88	27.44	4.87	2.43	7	205.80	288	3	4.41	373	537
0.5	30	146	84	4.85	68.60	12.31	6.16	17	514.50	720	8	8.83	834	1096
0.75	52	214	146	4.11	118.91	21.47	10.73	29	891.80	1249	13	13.24	1397	1780
1.0	75	319	210	4.25	171.50	31.05	15.53	42	1286.25	1801	19	17.65	1986	2496
1.25	90	300	252	3.33	205.80	37.20	18.60	51	1543.50	2161	23	22.25	2370	2962
1.50	120	534	324	4.45	264.60	47.94	23.97	65	1984.50	2778	30	26.70	3029	3762
CPT-4: 689972mE; 792656mN; 249m absl														
0.25	20	96	56	4.82	45.73	8.28	4.14	11	343	480	5	4.65	578	785
0.5	40	174	112	4.35	91.47	16.57	8.28	23	686	960	10	9.30	1090	1407
0.75	78	328	218	4.20	178.36	32.57	16.29	44	1338	1873	20	13.95	2063	2589
1.0	138	675	386	4.89	315.56	58.01	29.00	78	2367	3313	35	18.60	3600	4455
CPT-5: 690102mE; 793091mN; 250m absl														
0.25	15	68	42	4.50	34.30	6.15	3.08	8	257	360	4	4.44	449	630
0.5	35	148	98	4.22	80.03	14.45	7.23	20	600	840	9	8.88	962	1252
0.75	60	243	168	4.05	137.20	24.89	12.45	34	1029	1441	15	13.31	1602	2029
1.0	78	328	218	4.21	178.36	32.33	16.17	44	1338	1873	20	17.75	2063	2589
1.25	85	338	230	3.98	187.43	33.76	16.88	46	1406	1968	21	22.19	2164	2712
1.50	95	271	257	2.85	209.48	37.59	18.79	52	1571	2199	24	27.00	2411	3012
1.75	128	625	333	4.88	271.79	48.99	24.50	67	2038	2854	32	31.50	3109	3860

The obtained values of Q_c ranged from 28–138 kg/cm^2 (avg. 65 kg/cm^2), S_r varied from 46–675 kg/cm^2 (avg. 268 kg/cm^2), Q_{cn} is between 28 - 386 kg/cm^2 (avg. 177 kg/cm^2), F_R ranged from 2.85–4.89 (avg. 4.22), Q_{all} varied from 22.87–315.56 kN/m^2 (avg. 144.77 kN/m^2), UCS is in between 4.0–58.0 kN/m^2 (avg. 26.1 kN/m^2), C_u ranged from 2–29 kN/m^2 (avg. 13.1 kN/m^2), M-number varied from 6–78 (avg. 36), E_{square} is between 171.5–2369 kN/m^2 (avg. 1086 kN/m^2), E_{strip} ranged from 240–3313 kN/m^2 (avg. 1520 kN/m^2), N_{cor} varied from 3–35 (avg. 16), and σ_o is between 4.08–37.0 KN/m^2 (avg. 16.88 kN/m^2).

The allowable bearing pressure for strip (Q_{strip}) and square (Q_{square}) ranged from 321–3600 kN/m^2 (avg. 686.7 kN/m^2), and 474–4455 kN/m^2 (avg. 2132.2 kN/m^2) respectively. The geologic units showed for CPT 1 (0–1.2 m–clay; 1.2–1.5 m–silty clay to clay; 1.5–1.75 m–clayey silt to silty clay; 1.75–2.0 m–very stiff clayey soil; CPT 2 (0–0.5 m–clay; 0.5–0.75 m–silty clay to clay; 0.75–1.25 m–clay silt to silty clay; 1.25–1.75 m–sandy silt to clayey silt); CPT 3 (0–0.75 m–clay; 0.75–1.25 m–clayey silt to silty clay; 1.25–1.5 m–sandy silt to clayey silt; 1.5–1.6 m–very stiff clayey soil (hardpan); CPT 4 (0–0.75 m–clay; 0.75–1.0 m–silty clay to clay; 1.0–1.25 m–silty sand to sandy silt); CPT 5 (0–0.75 m–clay; 0.75–1.25 m–silty clay to clay; 1.25–1.5 m–clayey silt to silty clay; 1.5–1.75 m–sandy silt to clayey silt; 1.75–1.8 m–very stiff clayey soil (hardpan).

Consequently, the soil in the upper 2.0 m is predominantly clay/silty clay to clay, usually regarded as weak soil for most civil engineering construction. This agreed with the result of the VES, borehole sections, and grain size distribution, which identified the topsoil/subsoil as sandy clay, clay, clay/laterite respectively.

The average Q_c (65 kg/cm^2), Q_{all} of 144.8 kN/m^2 obtained can support light/medium weight foundation structure without excessive settlement. The refusal depths for the survey varied between 1–2.0 m and are usually terminated in very stiff clayey soil (hardpan). Using the values of CU, the soil, the consistency of the soils is in between soft to very soft. From the graph, the Q_C, M-Number, and Q_{all} increase with depth.

3.9. Geotechnical Parameters Modeling and Correlations

The obtained graphs for the parameters correlated are shown in Fig. 15. The obtained MDD/PI was correlated with soaked CBR determined from the laboratory and gives weak positive correlation (R^2) of 0.0046 and linear regression model (*Equation 13*):

$$CBR\ (soaked) = 0.0363x + 2.6216 \quad (13)$$

In this relationship, x = MDD/PI

The LL was plotted against coefficient of consolidation. This gives a regression model of *Equation 14*, with weakly positive correlations (R^2) of 0.0127.

$$Coefficient\ of\ consolidation = -1E\text{-}05x + 0.0102 \quad (14)$$

In these relationships, x = LL.

The relationship between PI and undrained shear strength/effective overburden, is shown by the regression model in *Equation 15*, with R^2 of 0.0074.

$$\frac{undrained\ shear\ strength}{effective\ overburden} = -0.0288x + 6.5013 \quad (15)$$

Where x is PI.

The correlation between dry density and angle of shearing gives *Equation 16*, with correlation coefficient of 0.4022.

$$Angle\ of\ shearing = -1.6004x + 37.458 \quad (16)$$

Where x is dry density

The plot of PI and angle of shearing gives correlation coefficient of 0.042, and model is presented in *Equation 17*.

$$Angle\ of\ shearing = -0.2365x + 14.55 \quad (17)$$

Where x is PI.

The relationship between suitability index and soaked CBR gives a weak positive correlation of 0.0968, and the regression model shown in *Equation 18*.

$$CBR\ (soaked) = 761.34x - 2.6129 \quad (18)$$

Where x is suitability index.

In addition, the obtained clay content was correlated with PI and gives weak positive correlation (R^2) of 0.0777 and linear regression model (*Equation 19*).

$$PI = 0.0805x + 18.176 \quad (19)$$

Where x is clay content.

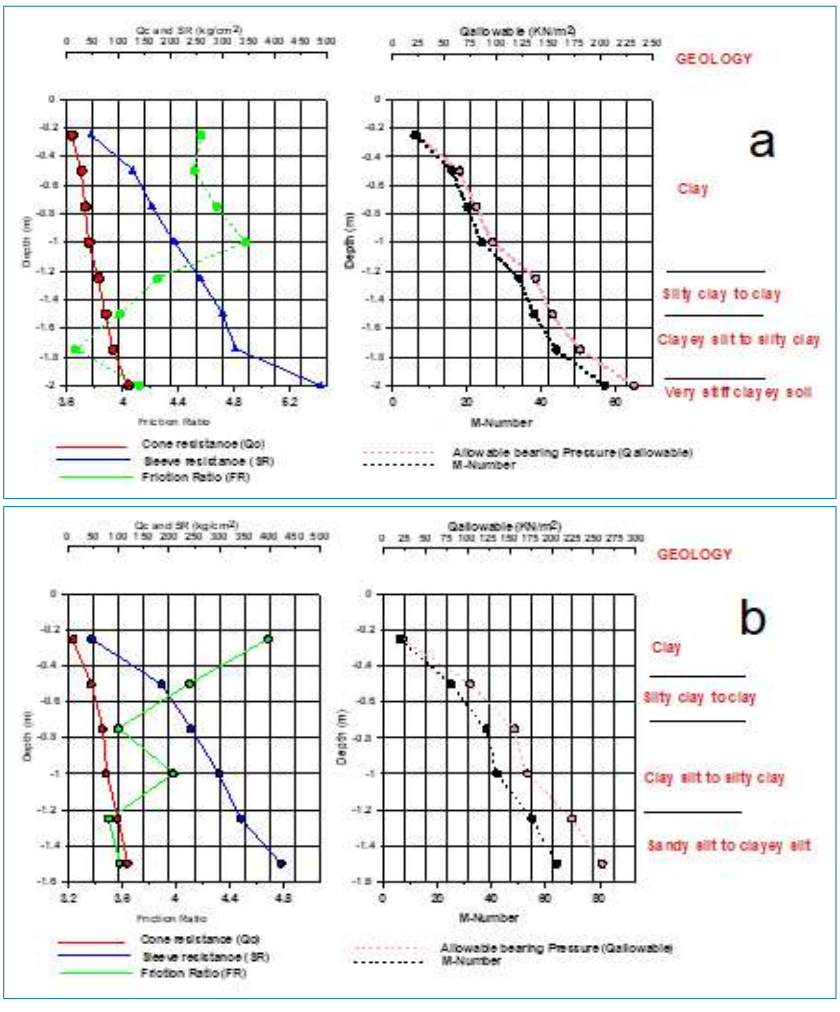

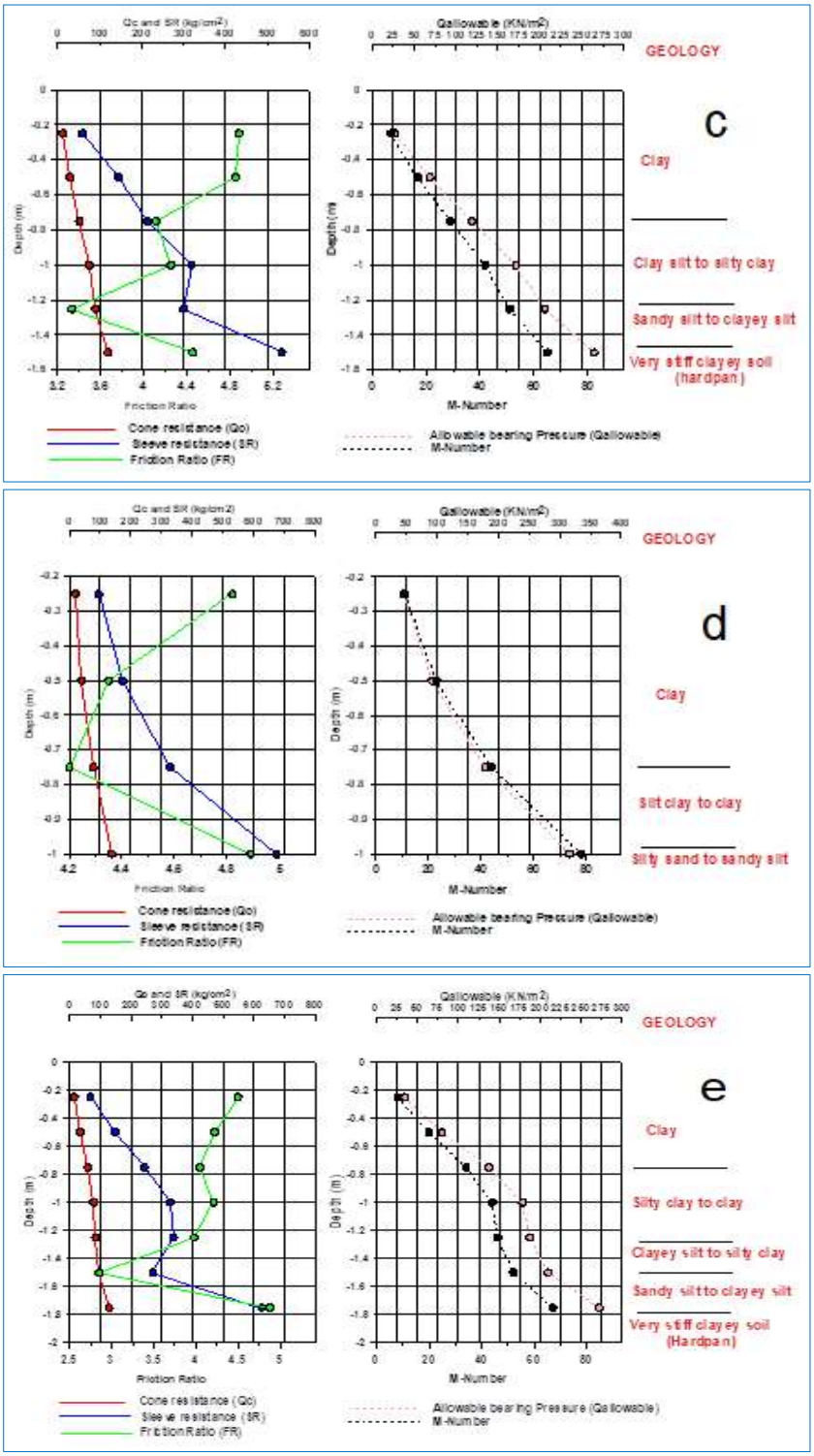

Fig. 14. The Interpreted CPT data obtained from study area, showing the plots of cone resistance, sleeve resistance, friction ratio, allowable bearing pressure, and M-Number with respect to depth for CPT 1-5, respectively

3.10. Implication for Varying Civil Engineering Construction

3.10.1. Pavement and Airfield

Pavement performance depend on subgrades that provides a uniform and sufficiently stiff, strong, and stable foundation for the overlying layers and adequate drainage that quickly remove water from the pavement structure before the water degrades the properties of unbound layers and subgrade (Weltman and Head, 1983; Brown, 1996).

The CBR test is used exclusively in conjunction with pavement design methods and the method of sample preparation and testing in pavement design, especially the soaked CBR value, regardless of site condition. However, CBR values depend not only on soil type but also on density, moisture content and, to some extent, method of preparation. The engineering properties of soil desired for foundation under highway and airfield should have adequate strength,

good compaction, adequate drainage, and acceptable compression and expansion properties. The design of flexible pavement is normally based on Group Index method or CBR method (George and Uddin, 2000; Brown, 1996; Wright, 1986). The drainage characteristics of the soil is poor/impervious with soaked CBR generally less than 10.

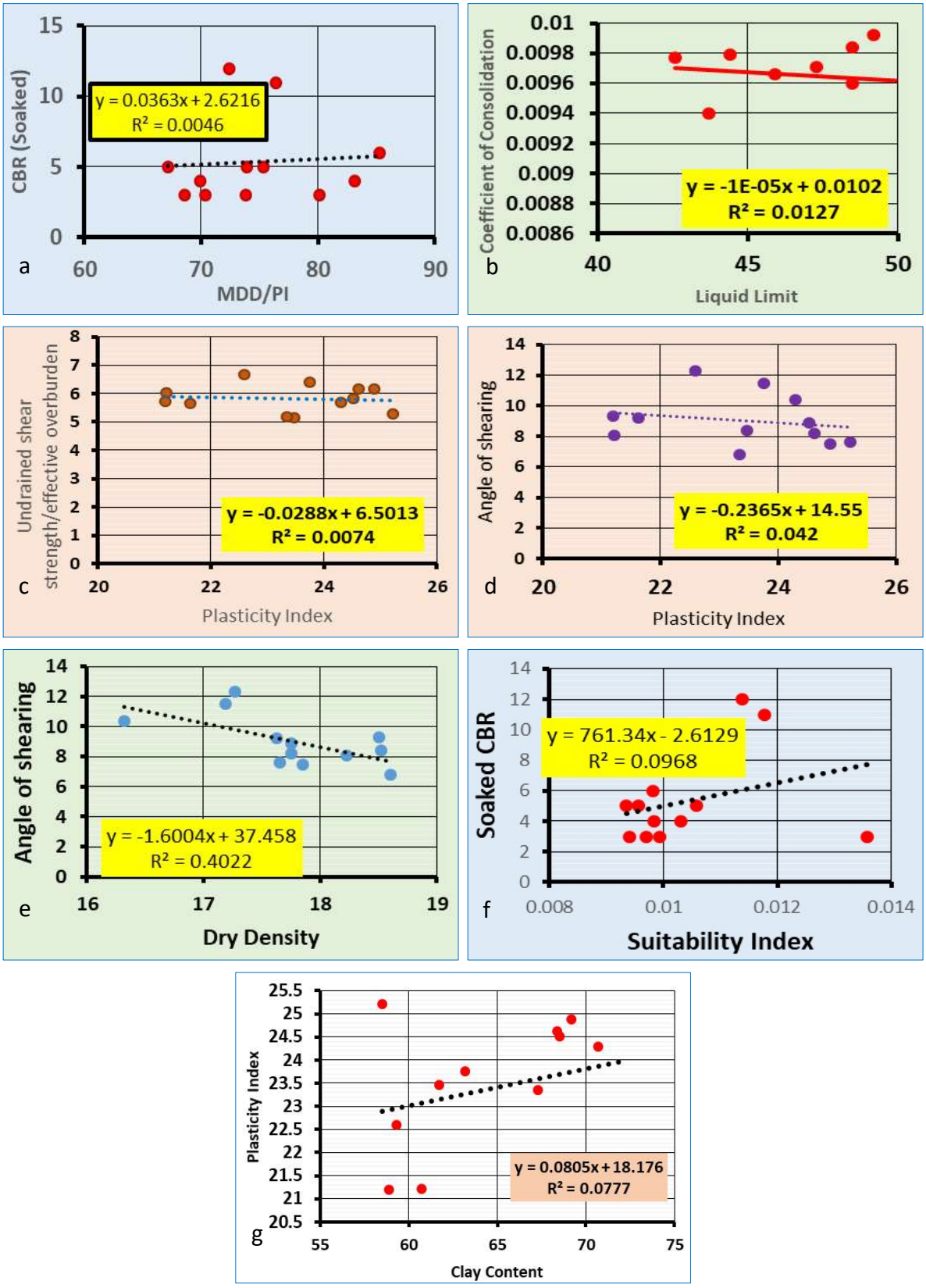

Fig. 15. Geotechnical parameters correlation for some of the engineering properties of the soils

Table 12. The Highway and foundation characteristics of the soil with expected settlements

Sample No.	Subgrade Rating		GI Class	Rec Thickness (mm)	Suitability Index	Bearing Capacity (kN/m²) Square Footing		Bearing Capacity (kN/m²) Round Footing		Settlement (mm)		
	USCS Class	AASHTO Class				Q_T	Q_A	Q_T	Q_A	Elastic	Consol	Total
OK-1	Poor to Fair	Poor	Poor	432	0.0093	926	308	924	308	3.83	22.70	26.53
OK-2	Poor to Fair	Poor	Poor	279	0.0118	1068	356	1066	355	3.65	24.62	28.27
OK-3	Poor to Fair	Poor	Poor	267	0.0114	1044	348	1042	347	3.58	25.02	28.6
OK-4	Poor to Fair	Poor	Poor	584	0.0097	999	333	998	333	3.83	20.09	23.92
OK-5	Poor to Fair	Poor	Poor	432	0.0106	944	315	941	314	2.62	23.32	25.94
OK-6	Poor to Fair	Poor	Poor	508	0.0098	962	320	960	320	4.98	23.62	28.6
OK-7	Poor to Fair	Poor	Poor	584	0.0099	1053	351	1051	350	3.86	25.22	29.08
OK-8	Poor to Fair	Poor	Poor	584	0.0136	977	326	975	325	4.88	23.92	28.8
OK-9	Poor to Fair	Poor	Poor	419	0.0098	1055	352	1053	351	4.65	25.12	29.77
OK-10	Poor to Fair	Poor	Poor	432	0.0096	892	297	889	296	3.51	22.39	25.9
OK-11	Poor to Fair	Poor	Poor	508	0.0103	1008	336	1005	335	3.55	24.42	27.97
OK-12	Poor to Fair	Poor	Poor	584	0.0094	951	317	949	316	4.68	23.52	28.2

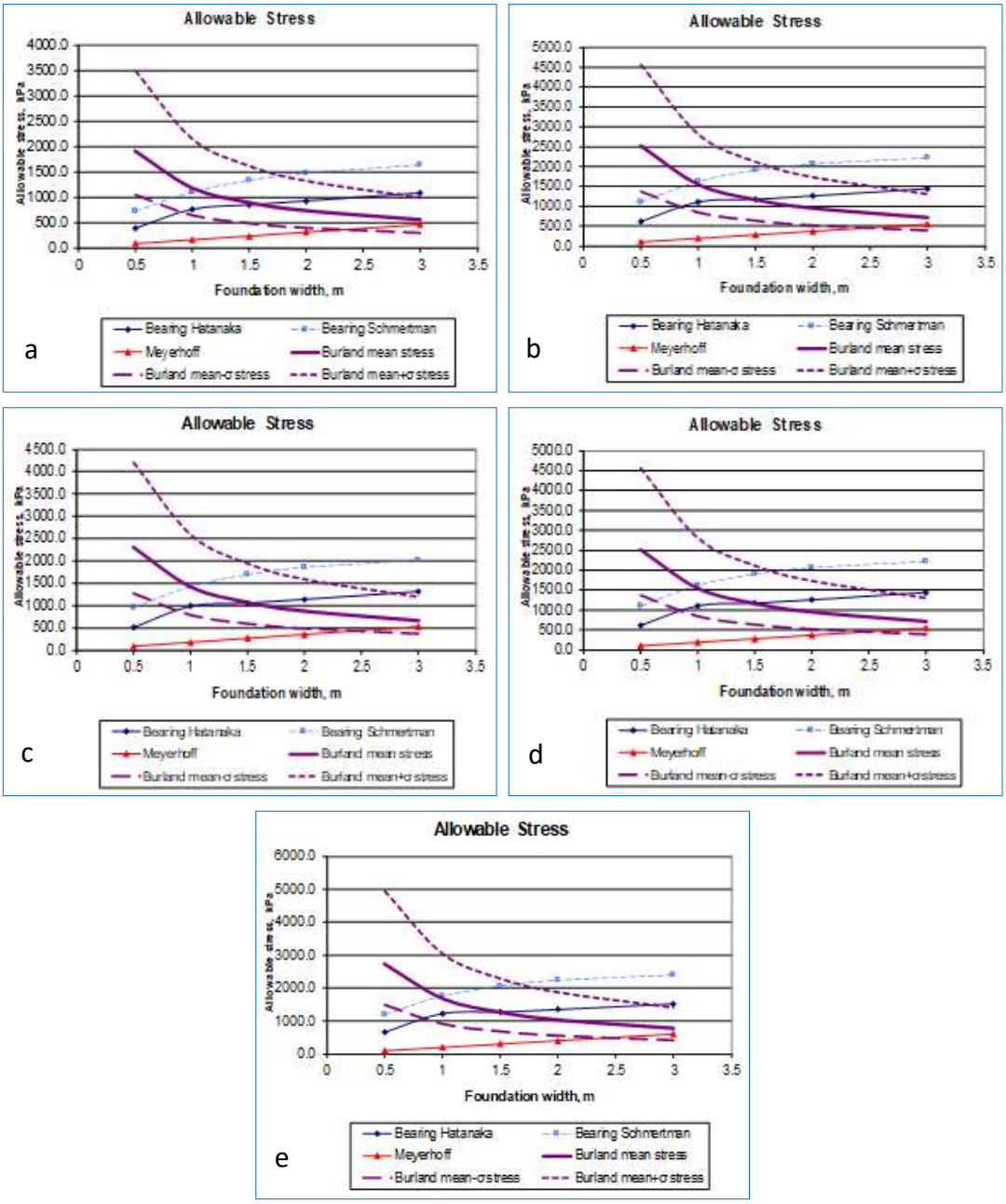

Fig. 16. Model graph of the bearing pressure and stresses for various footing width using CPT data for maximum allowable settlement of 25 mm

The AASHTO classification of the soil for subgrade is poor; and USCS as fair - poor (Table 12). AASHTO classification suitability of soils for pavement subgrades; the higher group numbers being progressively less suitable. A further refinement of the AASHTO system in this respect is the use of a group index (George and Uddin, 2000; Wright, 1986) to evaluate subgrade quality. From the result of the study, the GI ranged from 11-17 (avg. 14) corresponding to poor subgrade for highway construction, with expected recommended minimum -thickness of 267–584 mm (avg. 468 mm) obtained from design curves (Table 9). The average soaked CBR of the soils is 5 % which fell below 10 % recommended standard for subgrade, base or subbase. Thus, the soil is unsuitable for subgrade, base and sub-base courses.

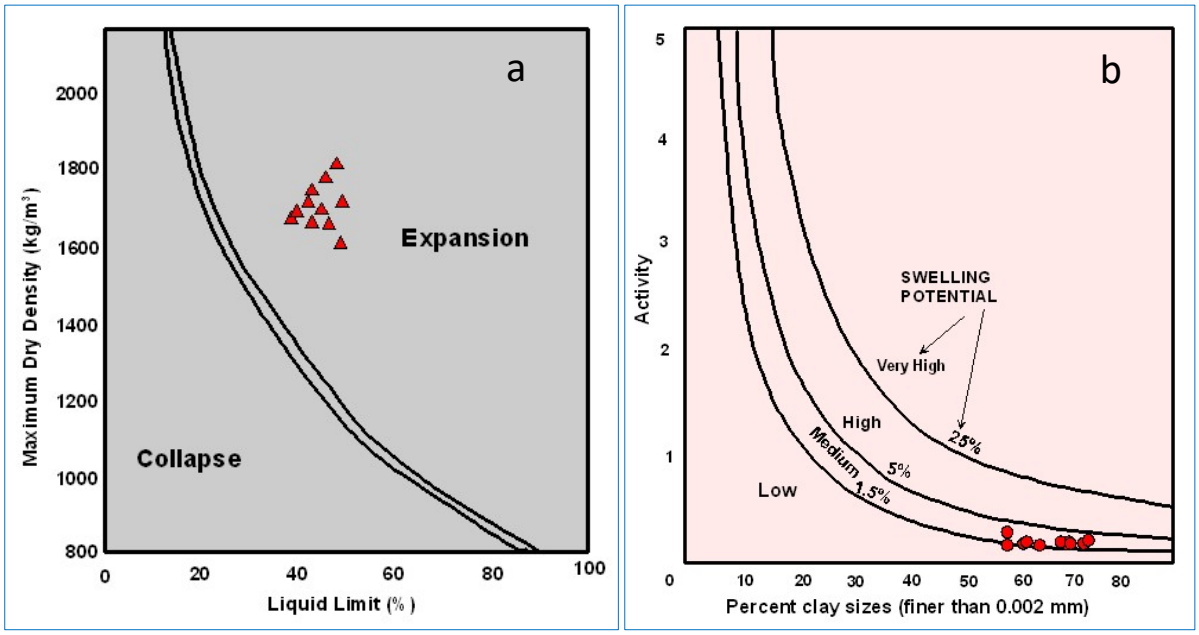

Fig. 17. Workability and swelling potential of the soil's classification chart for swelling potential (after Carter and Bentley, 1991; Holtz and Kovacs, 1981)

3.10.2. Building Foundation

The average allowable bearing capacity of the soil for square and round foundations varied from 297–56 kN/m^2 (avg. 330 kN/m^2) and 296–355 kN/m^2 (avg. 329 kN/m^2). The estimated immediate/elastic settlement ranged from 2.62–4.98 mm (avg. 3.96 mm); and consolidation settlement varied between 20.1–25.2 mm (avg. 23.7 mm). The total settlement obtained is in between 23.9–29.8 mm (avg. 27.6 mm) for structural pressure of 100 kN/m^2. These results showed that the soil exhibits more consolidation settlement than elastic, which implies that the soil behaves more of fine soil material.

The settlement of soils in response to loading can be broadly divided into two types: elastic settlement and time-dependent settlement. Elastic settlements are the simplest to deal with, they are instantaneous, recoverable, and can be calculated from linear elastic theory. Time dependent settlements occur in both granular and cohesive soils, although the response time for granular soils is usually short.

In addition to being time-dependent, their response to loading is non-linear, and deformations are only partially recoverable. Two types of time-dependent settlement are recognized. Primary consolidation results from the squeezing out of water from the soil voids under the influence of excess pore water pressures, generated by the applied loading. Secondary compression occurs essentially after all the excess pore pressures have been dissipated, that is, after primary consolidation is substantially complete. From the CPT result, the average allowable pressure was estimated to be 145 kN/m^2 for an average depth of 1.0 m. These bearing pressures are low and would only be suitable for light/medium weight structures, with adequate factor of safety.

The bearing (using Hatanaka and Uchida (1996), Mayne (2001), Schmertmann (1975) and Meyerhof (1956) equations) gave model bearing capacity with respect to foundation width as shown in Fig. 16. The deformation criterion was calculated using Burland and Burbridge (1984) equation. The applied factor of safety is 3.0, for maximum allowable settlement of 25.0 mm. However proper soil improvement methods (mechanical and/or chemical) must be adopted, since clay/plastic silt tends to undergo volume change when desiccated, to ensure that the settlement. Summarily the estimated settlement is above the standard 25 mm for building foundations of 100 kN/m^2.

3.10.3. Embankment

For satisfactory performance of an embankment material, the soil should have high stability and strength and be well graded; coarse grained (such as sand, gravel) is usually preferable to fine soil. The suitability index of the soils ranged from 0.0093–0.0136 (avg. 0.01). The USCS classification of the soil is CL which depicts soils of low stability; that can be used for impervious core for flood control structures. The

suitability index of the soil suggests an expanding not collapsible construction material, as shown also in Fig. 17 having medium swelling potential. The compaction characteristics of the soil are poor, while the drainage characteristics are poor to practically impervious. Thus, since the soils have high MDD at high OMC (avg. 1741 kg/m^3; 29 %) greater than 1500 kg/m^3, they are ordinarily considered suitable with stabilization (Upadhyay, 2015; Carter and Bentley, 1991; Bell, 2007). The American Association of State Highway and Transportation Official (AASHTO, 2006) classification of the fines in the samples as A-6/A-7-6. A-6 soil is typical of plastic clay having a high percentage passing 0.075 mm and usually characterized with high volumetric change between wet and dry states.

A-7-6 materials have high plasticity indices in relation to the liquid limits and are subject to extremely high-volume change. A-7-5 materials have moderate plasticity indices in relation to the liquid limits and may be highly elastic as well as subject to volume change. Therefore, the soils with A-7-6/A-6 fines can be placed at the bottom of embankment and remain in the top 0.5 m below subgrade in highway construction. Therefore, comparing the important soils parameters such as plasticity, compressibility, strength (shear), workability, and compaction characteristics, the soils are rated according to their utility for dams, canals, foundations, and highway in Table 10. The relative score given to the soil is in the order of desirability from 1 to 14 i.e., high to low respectively. The findings from this study also confirmed some earlier suggestions to the effect that the course the material, the greater generally is its strength and the finer the material, the worse are its engineering properties. Thus, from Table 13, the soil is generally fair/poor with an average suitability score of 8.

Table 13. Summary of desirability potential of the soil for various engineering uses

Various uses	Properties	Characteristics/relative suitability
Important engineering parameter/property	Permeability when compacted	Impervious
	Shear strength when compacted saturated	Fair
	Compressibility when compacted saturated	Medium
	Workability as construction material	Fair-poor
Earth fill dams	Rolled Earth fill dams (homogeneous embankment)	S: 7
	Rolled Earth fill dams (core/shell)	S: 7
Canal	Canal sections (erosion resistance)	S: 10
	Canal sections (compacted earth lining)	S: 8 (volume change critical)
Foundation	Foundations (where seepage is important)	S: 5
	Foundations (where seepage not important)	S: 11
Roadway	Roadway fills	S: 8
	Roadway surfacing	S: 7

4. Conclusions

Therefore, it can be concluded that the soils in the study are characterized by PI greater than 20 % and composed generally of sandy clay/clay soil (CL) with average % fines of 78.3. The depth to groundwater ranged from 2.2 m (in well)–18 m (in borehole). The depth to basement rock is between 8.2–31.5 m (avg. 20.9 m), indicating a moderate to deep weathering profile, able to support burial of engineering utilities such as mast, transformer, gadgets, etc. The soil is generally inactive type with predominant illite-montmorillonite clay mineralogy group, with activity of 0.36. Findings also showed that the soil is unsuitable for base and sub-base courses with CBR less than 7% and GI of 14 (avg.), with expected recommended minimum thickness of 79–140 mm (avg. 109 mm) obtained from design curves for flexible pavement. The average allowable bearing capacity of the soil for square and round foundations is 320 kN/m^2. The total settlement obtained is in between 23.92–29.77 mm (avg. 27.6 mm) for structural pressure of 100 kN/m^2. For embankment, the suitability index of the soil suggests an expanding not collapsible construction material.

Metamorphic rocks are widespread in the study area, some are outcropped while some are deep seated with the subsurface. However, it is expected for the rock to have very high compressive/shear strength, modulus of elasticity, high crushing strength, low deformability; and presumable bearing capacity of 4, 000–12, 000 kPa especially when fresh (FR), and can be in between 2500–8000 kPa when partly or slightly weathered (SW) and thus can be trusted in most construction works, especially as foundation and road stones, as Falowo (2015) reported high values for aggregate impact value, aggregate crushed value, point load strength test, unconfined compression test, and direct shear strength for the rock in northern area of the same geological province which are contemporaneous in history. Therefore, the rocks have high value as foundation constructions, aggregate in pavement, and building stone.

Conflict of Interest

The authors declare no conflict of interest exists in this publication.

References

AASHTO, 2006. Standard Specifications for Transportation Materials and Methods of Sampling and Testing, Parts I and II, American Association of State Highway and Transportation Officials, Washington, D.C.

Adejumo, S.A., Oyerinde, A.O., Akeem, M.O., 2015. Integrated geophysical and geotechnical subsoil evaluation for pre-foundation study of proposed site of vocational skill and entrepreneurship center at the polytechnic, Ibadan, SW, Nigeria. International Journal of Scientific & Engineering Research 6 (6), 910-917.

Adeoti, L, Ojo, A.O., Adegbola, R.B., Fasakin, O.O., 2016. Geoelectric assessment as an aid to geotechnical investigation at a proposed residential development site in Ilubirin, Lagos, Southwestern Nigeria. Arabian Journal of Geosciences 9, 338. https://doi.org/10.1007/s12517-016-2334-9.

Adewuyi, O.I., Philips, O.F., 2018. Integrated Geophysical and Geotechnical Methods for Pre-Foundation Investigations. Journal of Geology & Geophysics 7, 453. https://doi.org/10.4172/2381-8719.1000453.

Archana, P.M., Padma, K.R., 2016. Engineering and Geological Evaluation of Rock Materials as Aggregate for Pavement Construction. International Advanced Research Journal in Science, Engineering and Technology, Vol. 3, Special Issue 3, August 2016. https://doi.org/10.17148/IARJSET.

ASTM, 2006. Annual Book of ASTM Standards – Sections 4.02, 4.08, 4.09 and 4.13. ASTM International, West Conshohocken, PA.

Attewell, P.B., Farmer, I.W., 1988. Principles of engineering geology Principles of Engineering Geology. John Wiley & Sons, Inc, New York, 1045 pp. https://doi.org/101007/978-94-009-5707-7.

Bell, F.G., 1998. Environmental Geology: Principles and Practice. Blackwells, Oxford.

Bell, F.G., 2007. Engineering Geology Second Edition, Elsevier Limited.

Bell, F.G., 2004. Engineering Geology and Construction. Spon Press, London.

Brassington, R., 1988. Field Hydrogeology. Wiley, Chichester.

Brink, A.B.A., Parridge, J.C., Williams, A.A.B., 1992. Soil Survey for Engineering. Clare, Oxford, 3739g. pp. 1-22.

Brown, S.F., 1996. Soil mechanics in pavement engineering. Geotechnique 46, 383–426.

BS 1377, 1990. Methods of Tests for Soils for Civil Engineering Purpose, British Standard Institution HMSO London.

Burland, J.B., Burbidge, M.C., 1984. Settlement of foundations on sand and gravel, Proceedings of the Institution of Civil Engineers, Part 1, 1985, 78, Dec., 1325-1381.

Carter, M., Bentley, S.P., 1991. Correlations of soil properties, Pentech Press Publishers, London, 129pp.

Carter, M., Symons, M.W., 1989. Site Investigations and Foundations Explained. Pentech Press, London.

Cetin, K.O., Ozan, C., 2009. CPT-based probabilistic soil characterization and classification. Journal of Geotechnical and Geoenvironmental Engineering 135 (1), 84–107. https://doi.org/10.1061/(ASCE)10900241(2009)135:1(84).

Clayton, C.R.I., Simons, N.E., Matthews, M.C., 1996. Site Investigation: A Handbook for Engineers. Second Edition, Blackwell Scientific Publications, Oxford.

Coker, J.O., 2015. Integration of Geophysical and Geotechnical Methods to Site Characterization for Construction Work at the School of Management Area, Lagos State Polytechnic, Ikorodu, Lagos, Nigeria. International Journal of Energy Science and Engineering 1 (2), 40-48.

Coker, J.O., Makinde, V., Adesodun, J.K., Mustapha, A.O., 2013. Integration of Geophysical and Geotechnical Investigation for a Proposed New Lecture Theatre at Federal University of Agriculture, Abeokuta, South Western Nigeria. International Journal of Emerging Trends in Engineering and Development 3 (5), 338-348.

Craig, C., 1996. Advances in Site Investigation Practice. Thomas Telford Press, London.

Culshaw, M.G., Bell, F.G., Cripps, J.C., O'Hara, M., 1987. Planning and Engineering Geology. Engineering Geology Special Publication No. 4, Geological Society, London.

Douglas, B.J., Olsen, R.S., 1981. Soil classification using electric cone penetrometer. In: Norris GM, Holtz RD (eds) Proceedings of the symposium on cone penetration testing and experience, St. Louis, Mo., 26-30 October 1981. Geotechnical engineering division, American Society of Civil Engineers, New York, pp 209-227.

Ezenwaka, K.C., Ugboaja, A., Ahaneku, C.V., Ede, T.A., 2014. Geotechnical investigation for design and construction of civil infrastructures in parts of port Harcourt City of Rivers State, Southern Nigeria. The Int J Eng Sci 3: 74-82.

Fajana, A.O., Olaseeni, O.G., Bamidele, O.E., Olabode, O.P., 2016. Geophysical and geotechnical investigation for post foundation studies, Faculty of Social Sciences and Humanities, Federal University Oye Ekiti. FUOYE J Eng Tech 1: 2579-0617.

Falowo, O.O., Dahunsi, S.D., 2020. Geoengineering Assessment of Subgrade Highway Structural Material along Ijebu Owo – Ipele Pavement Southwestern Nigeria. International Advanced Research Journal in Science, Engineering and Technology 7 (4), 1-10. https://doi.org/1017148/IARJSET20207401.

Falowo, O.O., Olabisi, W., 2020. Engineering Geological and Geotechnical Site Characterization for Economic Design of Structures and Earthworks. Journal of Research and Innovation for Sustainable Society 2 (2), 43-60. https://doi.org/1033727/jriss202027:43-60.

Falowo, O.O., Ojo, O.O., Daramola, A.S., 2015. The use of magnetic survey in engineering site characterization. International Journal of Innovative Research and Development 4 (13), 74-85.

Falowo, O.O., 2019. Engineering properties of some basement rocks of Nigeria as Aggregate in Civil Engineering Pavement Construction. Asian Review of Environmental and Earth Sciences 6 (1), 28-37. https://doi.org/10.20448/journal.506.2019.61.28.37.

Federal Meteorological Survey, 1982. Atlas of the Federal Republic of Nigeria, 2nd Edition, Federal Surveys, 160pp.

Federal Ministry of Works and Housing, 1997. General Specifications for Roads and Bridges. Volume II. 145-284. Federal Highway Department: Lagos, Nigeria.

George, K.P., Uddin, W. 2000. Subgrade characterization for highway pavement design, final report. Jackson, MS: Mississippi Department of Transportation.

Griffiths, J.S., 2002. Mapping in Engineering Geology. Geological Society, London.

Hanna, T.H. 1985. Field Instrumentation in Geotechnical Engineering. Trans Tech Publications, Clausthal-Zellerfeld.

Hatanaka, M., Uchida, A., 1996. Empirical correlation between penetration resistance and effective friction of sandy soil. Soils & Foundations 36 (4), 1-9, Japanese Geotechnical Society.

Hawkins, A.B., 1986. Site Investigation Practice: Assessing BS 5930. Engineering Geology Special Publication No. 2, Geological Society, London.

Holtz, R.D., Kovacs, W.D., 1981. An Introduction to geotechnical engineering, Prentice Hall.

Hunt, R.E., 2005. Geotechnical engineering investigation handbook, second edition, Taylor and Francis.

Idornigie, A.I., Olorunfemi, M.O., Omitogun, A.A., 2006. Integration of Remotely Sensed and Geophysical data Sets in engineering Site Characterization in a Basement Complex area of Southwestern Nigeria. Journal Applied Sciences Research 2 (9), 541-552.

Iloeje, P.N., 1981. A new geography of Nigeria. Longman Nigeria Limited, Lagos.

Legget, R.F., 1973. Cities and Geology. McGraw Hill, New York.

Luna, R., Jadi, H., 2000. Determination of dynamic soil properties using geophysical methods Proc. 1st Int. Conf. on the Application of Geophysical and NDT Methodologies to Transportation Facilities and Infrastructure Geophysics (Federal Highway Administration, Saint Louis, MO) vol 3, pp 1-15.

Martin, F.J., Doyne, H.C., 1927. Laterite and lateritic soils in Sierra Leone. Journal of Agricultural Science 17, 530-547.

Matawal, D.S., 2012. The challenges of building collapse in Nigeria. In: Proceedings of National Technical Workshop on Building Collapse in Nigeria: curbing the incidences of building collapse in Nigeria, pp. 3-54.

Mayne, P.W., 2007. Cone penetration testing: a synthesis of highway practice. Project 20-5.Transportation Research Board, Washington, D.C. NCHRP synthesis 368.

McCann, D.M., Eddleston, D., Fenning, P.J., Reeves, G.M., 1997. Modern Geophysics in Engineering Geology. Engineering Geology Special Publication No. 12. Geological Society, London.

McDowell, P.W., ; Barker, R.D., Butcher, A.P., Culshaw, M.G., Jackson, P.D., McCann, D.M., Skipp, B.O., Matthews, S.L., Arthur, J.C.R., 2002. Geophysics in Engineering Investigations. Engineering Geology Special Publication No. 19, Geological Society, Construction Industry Research and Information Association (CIRIA), London.

McNally, G., 1998. Soil and Rock Construction Materials. Spon Press, London.

Meyerhof, G.G., 1956. Penetration tests and bearing capacity of cohesionless soils, Journal of the Soil Mechanics and Foundation Division 82 (SM1), 1-19.

Milson J., 2003. Field Geophysics: The Geological Field Guide Series. 3rd Ed., Published John Wiley and Sons Ltd. 88pp.

Moss, R.E.S., Seed, R.B., Olsen, R.S., 2006. Normalizing the CPT for overburden stress. Journal of Geotechnical and Geoenvironmental Enggineering 132 (3), 378-387. https://doi.org/10.1061/(ASCE)1090-0241(2006)132:3(378).

Nigeria Geological Survey, 1984. Geological Map of Southwestern Nigeria, Geological Survey Department, Ministry of Mines, Power and Steel, Nigeria.

Nigerian Geological Survey Agency, 2006. Geological and Mineral Map of Ondo State, Nigeria.

Ojo, J.S., Olorunfemi, M.O., Akintorinwa, O.J., Bayode, S., Omosuyi, G.O., Akinluyi, F.O., 2015. Subsoil Competence Characterization of the Akure Metropolis, Southwest Nigeria Journal of Geography, Environment and Earth Science International 3 (1), 1-14.

Olayanju, G.M., Mogaji, K.A., Lim, H.S., Ojo, T.S., 2017. Foundation integrity assessment using integrated geophysical and geotechnical techniques: Case study in crystalline basement complex, southwestern Nigeria. Journal of Geophysics and Engineering 14 (3), 675-690. https://doi.org/10.1088/1742-2140/aa64f7.

Osinowo, O.O., Falufosi, M.O., 2018. 3D Electrical Resistivity Imaging (ERI) for subsurface evaluation in preengineering construction site investigation. NRIAG Journal of Astronomy and Geophysics 7 /2), 309-317. https://doi.org/10.1016/j.nrjag.2018.07.001.

Oyedele, K.F., Olorode, D.O., 2010. On Site Investigation of Subsurface Conditions using Electrical Resistivity Method and Cone Penetration Test at 'Medina Brook Estate, Gbagada, Lagos, Nigeria, World Applied Science Journal 11 (9), 1097-1104.

Prentice, J.E., 1990. Geology of Construction Materials. Chapman and Hall, London.

Reynolds, J.M., 2004. An Introduction to Applied and Environmental Geophysics. Second Edition, Wiley, Chichester.

Robertson, P.K., 1990. Soil classification using the cone penetration test. Canadian Geotechnical Journal 27, 151-158. https://doi.org/10.1139/t90-01.

Rogers, J.D., 2006. Subsurface exploration using the standard penetration test and the cone penetrometer test. Environmental and Engineering Geoscience 12 (2), 161-179. https://doi.org/10.2113/12.2.161.

Roy, S., Bhalla, S.K., 2017. Role of geotechnical properties of soil on civil engineering structures. Resources and Environment 7 (4), 103-109. https://doi.org/10.5923/j.re.20170704.03.

Rungroj, A., Mark, E.E., 2015. Application of 2D electrical resistivity tomography to engineering projects: Three case studies. Songklanakarin Journal of Science and Technology 37 (6), 675-681.

Sanglerat, G., 1972. The penetration and soil exploration, Development in geotechnical engineering, Elsevier Scientific Publishing, New York.

Schmertmann, J.H., 1975. Measurement of insitu shear strength, keynote lecture, Proceedings of the conference on in-situ measurement of soil properties, June 1-4, 1975, vol. II, American Society of Civil Engineers.

Sharma, P.V., 1997. Environmental and Engineering Geophysics. Cambridge University Press, Cambridge, USA. https://doi.org/10.1017/CBO9781139171168.

Simons, N.E., Menzies, B.K., Matthews, M.C., 2001. A Short Course in Geotechnical Site Investigation. Thomas Telford Press, London.

Smith, M.R., and Collis, L., 2001. Aggregates: Sand, Gravel and Crushed Rock Aggregates. Third Edition. Engineering Geology Special Publication No. 9. Geological Society, London.

Soupios, P.M., Georgakopoulos, P., Papadopoulos, N., Saltas, V., Andreadakis, A., Vallianatos, F., Sarris, A., Makris, J.P. 2007. Use of engineering geophysics to investigate a site for a building foundation. Journal of Geophysics and Engineering 4 (1), 94-103. https://doi.org/10.1088/1742-2132/4/1/011.

Upadhyay, A.K., 2015. Soil and Foundation Engineering, Second Edition, S.K. Kataria & Sons New Delhi, India, 349 pp.

Utgard, R.O., McKenzie, G.D., Foley, D., 1978. Geology in the Urban Environment. Burgess, Minneapolis.

Wright, P.H., 1986. Highway Engineering, Sixth Edition. John Willey and Sons: New York, NY.

Weltman, A.J., Head, J.M., 1983. Site Investigation Manual. Construction Industry Research and Information Association, Special Publication No. 25, London.